TAMPEREEN TEKNILLINEN YLIOPISTO
TAMPERE UNIVERSITY OF TECHNOLOGY

Merja Puurtinen

Precordial Bipolar Leads for Mobile ECG Applications

Julkaisu 1067 • Publication 1067

Tampere 2012

Tampereen teknillinen yliopisto. Julkaisu 1067
Tampere University of Technology. Publication 1067

Merja Puurtinen

Precordial Bipolar Leads for Mobile ECG Applications

Thesis for the degree of Doctor of Science in Technology to be presented with due permission for public examination and criticism in the Rakennustalo Building, Auditorium RG202, at Tampere University of Technology, on the 21st of September 2012, at 12 noon.

Tampereen teknillinen yliopisto - Tampere University of Technology
Tampere 2012

ISBN 978-952-15-2896-5 (printed)
ISBN 978-952-15-2924-5 (PDF)
ISSN 1459-2045

ABSTRACT

Advances in measurement technology and wireless signal transfer have enabled the design of new, smaller and portable—even plaster-like—electrocardiographic (ECG) measurement devices that enable patient monitoring at home or in emergency situations. The development of new, miniaturized biomedical sensors has opened up possibilities for their application, but also set new demands on signal analysis and interpretation. In particular, the new small wireless systems often utilize bipolar electrodes that have a shorter interelectrode distance (IED) and different electrode locations from those of the standard 12-lead system. This affects the quality and the information content of the signal. The general objective of this thesis was to evaluate the performance of short IED precordial bipolar ECG leads and to determine their optimal location.

This thesis adopted three methods to assess the properties of new bipolar precordial ECG leads: modeling, body surface potential map (BSPM) data, and exercise ECG data. First, two realistic, three-dimensional (3D) thorax models and lead field analysis were used to evaluate whether modeling of the measuring sensitivity of ECG leads could be used as a tool for designing new ECG leads. Second, BSPM data was used to study whether short-distance bipolar leads (IED approximately 6 cm) provide an ECG signal that is adequate for clinical utilization. Third, BSPM data was used to define where a bipolar ECG lead should be located in order to maximize the ECG signal strength within healthy subjects. Finally, the value of bipolar leads for diagnosing two major cardiac conditions—left ventricular hypertrophy (LVH) and coronary artery disease (CAD)—was assessed.

It was found that the modeled measuring sensitivity corresponds to the changes in actual ECG signal strength, so modeling can be useful, especially in cases where in vivo measurements are impossible such as in designing implantable applications. Based on ECG data from 236 healthy subjects, all studied bipolar ECG leads with a short IED (approximately 6 cm) provided a detectable signal when compared to a low noise level of 15 μV and considering the P-wave as the smallest parameter. The optimal location of the bipolar lead was diagonally near the chest electrodes of the standard precordial leads V2, V3, and V4 (to maximize QRS amplitude), or above the chest electrodes of leads V1 and V2 (to maximize P-wave amplitude). In the selected clinical applications, LVH and CAD, the performance of bipolar leads was surprisingly good. In differentiating LVH (n=305) and healthy subjects (n=236), the performance of a correctly positioned small bipolar lead was similar to that of the traditional Sokolow-Lyon method. When differentiating CAD (n=255) patients from non-CAD (n=126) or low-likelihood of CAD (n=198) subjects, the overall performance of bipolar lead CM5 corresponded to that of standard lead V5.

These results indicate that short IED bipolar leads provide a signal that is adequate for clinical use. Furthermore, the performance of these leads was shown to be similar or even superior to that of the commonly used standard leads. It can be concluded that when correctly positioned, short IED bipolar leads are useful and can give additional value for clinical diagnostics. These results provide promising information on the applicability and potential of short IED bipolar ECG leads, and demonstrate that they are worth developing further.

ACKNOWLEDGEMENTS

This work was carried out at Tampere University of Technology, Department of Biomedical Engineering.

I am very grateful to my supervisors, Professor Jari Hyttinen and Professor Jari Viik, for their guidance and support throughout the research; their encouraging attitude and expertise in the field have been invaluable. I would also like to thank Professor Jaakko Malmivuo for his constructive remarks on the modeling research.

I am indebted to all my co-authors for their valuable contributions to my research over the years. I would also like to thank all my colleagues at the Department of Biomedical Engineering for the inspiring and positive working environment. I would especially like to thank Juho Väisänen, PhD, for helping me in the analysis of clinical material and in designing the LVH research. I am also grateful to Pasi Kauppinen, PhD, for modifying the thorax models to make them suitable for my research. Further, I wish to thank our department's secretary, Soile Lönnqvist, for taking such a good care of us and for giving me fruitful chili trees.

It was an honor to have Cardiologist Helena Hänninen, MD, PhD, Helsinki University Hospital, Division of Cardiology, and Professor Tapio Seppänen, PhD, University of Oulu, Department of Computer Science and Engineering as examiners of this thesis. I am grateful for their constructive comments and the effort and time they spent on my thesis. I am also privileged to have Professor Leif Sörnmo, Lund University, Faculty of Engineering, as an opponent of this thesis.

I am indebted to Professor Friedrich Kornreich, MD, for providing the clinical BSPM data. I am also grateful to the members of FINCAVAS project, for providing the exercise ECG data and for contributing to the publication regarding CAD.

The financial support of the Academy of Finland, the Finnish Cultural Foundation, the Pirkanmaa Regional Fund of the Finnish Cultural Foundation, the Instrumentarium Foundation, and the Kordelin foundation is gratefully acknowledged.

Finally, I owe my warmest thanks to my family, to my closest friends, and to my love Jarkko. They have encouraged me at all times during this thesis project as well as during my "endless" studies. All the support they have provided me over the years was the greatest gift anyone has ever given me.

Tampere, July 2012
Merja Puurtinen

TABLE OF CONTENTS

LIST OF ORIGINAL PUBLICATIONS

[I] Puurtinen, M., Viik, J., Takano, N., Malmivuo, J., Hyttinen, J. (2009) Estimating the measuring sensitivity of unipolar and bipolar ECG with lead field method and FDM models. Computer Methods and Programs in Biomedicine, 94:161-167.

[II] Puurtinen, M., Viik, J., Hyttinen, J. (2009) Best electrode locations for a small bipolar ECG device: signal strength analysis of clinical data. Annals of Biomedical Engineering, 37(2):331-336.

[III] Puurtinen, M., Väisänen, J., Viik, J., Hyttinen, J. (2010) New precordial bipolar electrocardiographic leads for detecting left ventricular hypertrophy. Journal of Electrocardiology, 43(6): 654-659.

[IV] Puurtinen, M., Nieminen, T., Kähönen, M., Lehtimäki, T., Lehtinen, R., Nikus, K., Hyttinen, J., Viik, J. (2010) Value of leads V4R and CM5 in the detection of coronary artery disease during exercise electrocardiographic test. Clinical Physiology and Functional Imaging, 30(4):308-312.

AUTHOR'S CONTRIBUTION

The aim of Publication I was to evaluate whether modeling the electrode's measuring sensitivity with 3D thorax models predicts the signal strength in actual ECG data. Publication II concentrated on defining the optimal locations for a small bipolar ECG device with clinical BSPM data. The concepts of validating the modeling method with clinical BSPM data and optimizing the location for a small bipolar ECG device were formulated with Professor Jari Hyttinen. Otherwise, the author designed the studies, performed the calculations, and analyzed the results. The author also wrote the papers, while receiving valuable comments from the co-authors.

Publication III concerned a performance evaluation of new, small bipolar leads in LVH diagnosis. The methods were implemented, the results were analyzed, and the paper was written with Juho Väisänen, PhD, with equal contribution. The work was conducted under the supervision of Professor Jari Viik, and comments on the paper were received from all co-authors.

Publication IV concerned testing the value of new leads—right precordial V4R and bipolar CM5—in CAD detection with an exercise ECG. The author designed the study with Professor Jari Viik, who presented the idea of evaluating the performance of these additional leads. In this publication, the author implemented the statistical analysis of the ECG data, prepared the results, and wrote the paper, while receiving comments from all co-authors.

LIST OF ABBREVIATIONS

3D	Three dimensional
BSN	Body sensor network
BSPM	Body surface potential map
CAD	Coronary artery disease
CT	Computed tomography
ECG	Electrocardiogram, Electrocardiography
EMG	Electromyogram
FDM	Finite difference method
HR	Heart rate
ICM	Insertable cardiac monitor
IED	Interelectrode distance
ISM	Industrial-Scientific-Medical
LA	Left arm
LL	Left leg
LVH	Left ventricular hypertrophy
LLC	Low likelihood of CAD
MI	Myocardial infarction
MSD	Mean square difference
MR	Magnetic resonance
PDA	Personal digital assistant
RA	Right arm
RF	Radio frequency
ROC	Receiver operating characteristic
SD	Standard deviation
S/N	Signal to noise
SPECT	Single-photon emission computed tomography
VHM	Visible human man
WCT	Wilson’s central terminal

1. INTRODUCTION

The aim of this thesis is to evaluate the performance and find the optimal location for new bipolar ECG leads with a short interelectrode distance (IED). Cardiac activity is traditionally recorded with the standard 12-lead ECG system; however, the trend in healthcare is towards mobile, minimally obtrusive, individualized health services. Thus, there is an increasing interest in developing alternative electrode locations for physiological monitoring. As electronics become miniaturized and implantable devices are developed, new possibilities for long-term measurement are opened up in areas such as emergency care and remote monitoring. A variety of commercialized, mobile ECG systems have emerged over the last decade, including the chest-worn heart-rate belts by Polar and Suunto for the wellness and lifestyle market (Polar, Suunto). Small, handheld ECG applications include those developed by BlackBerry/Vodafone, the Apple iPhone ECG System developed by Alivecor and Oregon Scientific, and Omron HeartScan (BlackBerry, AliveCor, Omron). In addition, several devices for remote, wearable, or continuous ECG monitoring have been developed for research purposes.

Mobile and continuous ECG recording could be especially useful for individuals with a risk of heart problems, as it enables cardiac activity to be monitored unobtrusively in the home environment. In addition, remote monitoring enables health providers to access data in real time and possibly detect paroxysmal events. Urbanization, ageing, and lifestyle changes make chronic and non-communicable diseases—including cardiovascular disease—increasingly important causes of morbidity and mortality (WHO 2008). Finnish statistics show that as the population ages, ischemic heart diseases are becoming an increasingly widespread cause of death. In 2009, ischemic heart disease was the direct cause of death in 22% of all cases in the Finnish population (Statistics Finland). The main cause of ischemia in the heart muscle is coronary artery disease (CAD). In addition, left ventricular hypertrophy (LVH) is a potent, independent predictor of cardiovascular events, particularly in hypertension, in

which it dramatically increases the risk of stroke, coronary heart disease, and heart failure. The importance of diagnosing LVH has increased in recent years with the recognition that hypertrophy can be reversed and the adverse clinical outcomes delayed (Mathew 2001; Okin 2003). Hence, an early diagnosis of cardiac diseases such as LVH or CAD is important when it comes to treating the condition and delaying or preventing adverse clinical outcomes.

Remote home monitoring in everyday life could give additional tools for the early detection and prevention of cardiac diseases. In this vein, research and development related to wearable and implantable ECG recorders has been emerging over the past decade. Wearable devices can enhance the user's comfort and enable monitoring of the patient at home instead of in the hospital. Thus, unnecessary hospitalizations can be avoided, which again will reduce healthcare costs. Another benefit is that by applying new measurement devices, we can possibly enhance diagnostic accuracy and ensure that those who need urgent care get it as quickly as possible. In addition, sophisticated monitoring and communication systems can enable interaction between patient and healthcare professional at any time it is needed. All of these issues are of interest for future healthcare.

Wearable ECG monitors often require a shorter IED and different electrode locations than those of the traditional 12-lead system. Both applying new measurement configurations and reducing the IED affect the morphology and amplitudes of the measured signals, thus having an impact on diagnostics. For this reason, it is crucial to evaluate the performance of short-distance bipolar leads as candidates for wearable electrode leads, and to study how the electrode location and orientation influence the recorded signal. Modeling tools offer one means of studying the behavior of physiological signals.

Modeling has been used in a variety of applications in electrocardiology, ranging from the earliest homogeneous thorax ECG models used by Frank (Frank 1954; Frank 1956) to the development of implantable defibrillators (Gale 1994). The main benefit of modeling is that it enables phenomena to be investigated when it would be too tedious or impossible to study them using in vivo trials. Modeling also provides the possibility to study the sensitivity distributions of bioelectric measurements. This could be useful in designing measurement devices for conditions where the changes appear in a certain area of the cardiac muscle, such as in LVH or myocardial infarction (MI).

Another way of testing new electrode locations is by utilizing body surface potential maps (BSPM), which provide multielectrode ECG signals. BSPMs contain diagnostic information not present in conventional lead systems, and offer the possibility to analyze signals in several locations on the body surface. BSPMs have been used, e.g.,

to identify the best ECG leads for diagnosing acute myocardial ischemia or LVH (Kornreich 1988; Kornreich 1991; Kornreich 1998; Oikarinen 2004; Kornreich 2008), or determining the optimal locations for a small implantable ischemia monitor (Burke 2003; Song 2004; Arzbaecher 2006). When designing new, small, wearable or wireless ECG measurement systems, BSPM databases provide a good way to test new electrode locations with different subjects.

All in all, mobile and wearable ECG devices have been available for a while, but their additional value is marginal if we do not know where the recording electrodes should be placed to obtain a strong, reliable ECG signal. There is a lack of extensive studies on signal quality and robustness, as well as the optimal lead location, for new, small ECG measurement systems. The aim of this thesis is to investigate the performance of and determine the optimal location for closely spaced bipolar ECG leads that can be used in wireless, wearable, or even implantable ECG recorders. The study population included both healthy subjects and subjects with LVH or CAD. The results of this thesis provide new information on the applicability of novel bipolar ECG leads and the possibilities that they offer for future healthcare.

2. OBJECTIVES OF THE STUDY

The general objective of this thesis was to evaluate the performance of new, short IED precordial bipolar ECG leads and to determine their optimal location. First, these new leads were modeled; they were then studied in relation to an ECG BSPM database of normal subjects. Finally, the value of the new bipolar leads in the detection of two main cardiovascular diseases, LVH and CAD, was assessed.

The specific aims were as follows:

1. To evaluate whether modeling the sensitivity of ECG leads with realistic thorax models could be used as a tool for designing new ECG leads [I];

2. To determine whether short-distance bipolar ECG leads can provide an ECG signal that is adequate for clinical utilization [II];

3. To study where the new bipolar lead should be located in order to obtain the optimal ECG signal strength within healthy subjects [II];

4. To assess the value of new bipolar leads in diagnosing LVH and CAD [III and IV].

3. REVIEW OF THE LITERATURE

This chapter comprises a review of the literature with an emphasis on wireless ECG applications. In addition, the methods adopted in this thesis—modeling, BSPM, and exercise testing in electrocardiology—are introduced. Finally, the two cardiovascular diseases addressed in this thesis, specifically CAD and LVH, are briefly described.

3.1 Electrocardiography and wireless applications

Electrocardiography (ECG) is a tool that measures the electrical activity generated by the heart. During each heartbeat in a healthy heart, a wave of depolarization is triggered by the cells in the sinoatrial node; this spreads out through the atrium, passes through the atrioventricular node, and then spreads all over the ventricles. This is followed by repolarization. The recorded tracing is called an electrocardiogram (ECG), and this typically comprises of the following waves: the P-wave, representing atrial depolarization; the QRS complex, representing ventricular depolarization; and the T-wave, representing ventricular repolarization (Figure 1). Because the body acts as a volume conductor, this electrical activity generated by the heart can be measured with electrodes placed on the body.

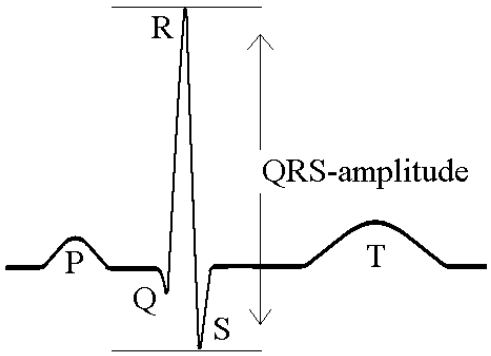

Figure 1. Normal electrocardiogram.

The ECG is traditionally recorded with the standard 12-lead system, which comprises six chest and six limb leads. The word *lead* refers to the voltage difference between the measuring electrode and the reference. The chest leads V1-V6 are unipolar, with Wilson's central terminal (WCT), which is the average of the limb electrode potentials, as a reference. Three of the limb leads are bipolar (I-III), measuring the potential difference between two electrodes, and another three are augmented unipolar leads (aVR, aVL, aVF), where the reference for the measurement electrode is the average of two other limb leads. The number of leads and the electrode placement has remained the same for over a half century, although the technology for measuring physiological signals has developed rapidly. The standard 12-lead system ECG is an invaluable tool, but new wearable and implantable devices offer new means of recording ECG signals for different applications. The American College of Cardiology (ACC) and the American Heart Association (AHA), in collaboration with the North American Society for Pacing and Electrophysiology, have developed guidelines for the use of ambulatory ECG (Crawford 1999). Several wireless, mobile, and wearable systems have been developed over the last decade; these are discussed below.

Wireless ECG

The origin of telemetric cardiac monitoring goes back to the early 1960s, when the clinical use of Holter monitors began. The Holter monitor is named after physicist Norman J. Holter, and the term refers to a portable device used to monitor bioelectrical signals. It is widely employed in electrocardiology for long-term, continuous monitoring of cardiac activity, and is usually worn for 24–48 hours during normal activity. Holter monitors have three to seven wires, depending on the model, and they can be used for recording unipolar or bipolar signals. Many new wearable and portable measurement systems use bipolar leads, meaning that the signal is detected between two recording electrodes. One well-known example of a wearable device is the heart rate (HR) monitoring belt, which has become widespread and a daily routine for many athletes.

The miniaturization in electronics and advances in signal transfer have enabled the development of small, plaster-like devices that include the measurement electronics and wireless transfer for measuring ECG. The IED used in the following devices corresponds to that studied in this thesis. Fensli et al. (Fensli 2004) introduced a small (70 x 35 x 18 mm) ECG sensor with an IED of 3 cm. The device utilizes wireless radio frequency (RF) transmission (Nordic VLSI; (NordicSemiconductor)) to a personal digital assistant (PDA), and provides 5 hours of operation. Another plaster-like device has been created by Munshi et al. (Munshi 2008), whose device measures 55 x 23 mm (IED = 5 cm) and utilizes wireless ZigBee (ZigBee) transmission. Russel et al. introduced an electrode assembly of three recording electrodes (IED = 2.48 cm) measuring less than 10 cm in its largest dimension (Russell 2007). This early prototype

of the monitor by Philips Medical Systems was capable of collecting 15 hours of ECG on three channels.

Another device of three electrodes was recently introduced by Trobec et al. (Trobec 2010). Their device used three wireless body electrodes (WBE) and bipolar configurations (IED = 5 cm) to synthesize the standard 12-lead ECG. The researchers reported that the 12 synthesized signals were similar to those of the simultaneously measured 12-lead ECG. Their device used the SimpliciTi (SimpliciTi) transfer protocol, and an operation time of 100 hours was reported. Another application using three wireless ECG electrodes was introduced by Chiu et al. They showed that a three-lead ECG from closely (10 cm) spaced wireless electrodes, located in the area of standard 12-lead system chest electrodes, was similar to the signal recorded from standard leads I, II, and III (Chiu 2011). The researchers chose the electrode location based on our previous findings in publication [I]. Among the commercialized wireless electrode systems, there is also an example benefiting from plaster-like ECG: the CardioPatch by Novosense (Novosense). This is a fully integrated unit of 4 cm in diameter, containing electrodes, an ECG amplifier, and a radio transmitter. CardioPatch transmits the ECG signal over 24 hours to the CardioBase receiver.

Signal transfer and wireless sensor networks

The developed wireless ECG recorders utilize a variety of different protocols for signal transfer. In general, the device should be able to work in a license-free industrial-scientific-medical (ISM) band, without interfering with other devices in the same frequency range. In addition, the data transmission rate is an important concern. Considering these factors, selected transmission protocols have been utilized in wireless ECG development, including Bluetooth, ZigBee, sub 2.4 GHz and 2.4 GHz transceivers, and Wibree. Bluetooth is one of the most traditional choices, as its main advantages are small size, low prize, multi-user capability, and simplified setup. However, ZigBee has certain advantages over Bluetooth, such as lower price and favorable power consumption for a wider coverage area. The ZigBee protocol has been utilized in many body sensor networks (BSNs), including Moteiv. Moteiv was founded at the University of California, Berkeley, with a focus on robustness and application building for wireless sensor networks.

Some projects have preferred a sub 2.4 GHz band for RF transmission, including Mica2 and Mica2Dot, both developed at University of California, Berkeley. This transmission protocol has been utilized, e.g., by Fulford-Jones et al. (Fulford-Jones 2004) in developing ECG on Mica2. This group has been working with the CodeBlue initiative at Harvard University (Malan 2004), which has also developed VitalEKG, a collection of software components that allow for the capture and wireless transmission of heart activity traces. In general, Code Blue is a wireless infrastructure intended for

deployment in emergency medical care, integrating low-power, wireless vital sign sensors, PDAs, and PC-class systems. Similarly, researchers at the MIT Media Lab have developed MIThril, a wearable computing platform compatible with both custom and off-the-shelf sensors (DeVaul 2003). MIThril includes ECG, skin temperature, and galvanic skin response (GSR) sensors. Other medical applications based on wireless sensor networks include the scalable medical alert response system (SMART), MobiHealth, and CardioNet (SMART, MobiHealth, CardioNet). Gyselinckx et al. have published an overview of the potential and challenges of using body area networks for cardiac monitoring (Gyselinckx 2007).

Mobile and handheld ECG

Recently, a range of mobile or handheld ECG applications has also been emerging. The BlackBerry mobile ECG application runs under the network of Vodafone, and the aim is to enable physicians to read the ECG reports of different patients remotely on their BlackBerry device (BlackBerry). Accordingly, Alivecor and Oregon Scientific have developed an ECG system that uses an Apple iPhone 4 and an iPhone ECG case containing electrodes for recording ECG (AliveCor). Another handheld device that records one-lead ECG is Cardio24 mobile palmtop ECG and InstantCheck mobile ECG by Davita (DAVITA). Generally, in these applications, the ECG signal is recorded by placing thumbs on the electrodes and the device records an ECG signal that corresponds to the standard lead I. Another option is to place the device directly on the chest, in which case the recorded bipolar lead is similar to the leads studied in this thesis. One commercial device benefiting from this measurement technique is Omron Heartscan Screening and Self-Monitoring of cardiac events (Omron).

Wearable applications

Wearable systems may be defined as mobile electronic devices that can be unobtrusively embedded in the user's outfit as part of his or her clothing or as an accessory. The conventional method for recording ECG is to use electrodes (usually Ag-AgCl) attached to the body. However, the development of textile technology has produced fibers and yarns with specialized electrophysical properties. These textile materials enable fabric sensors to be integrated into clothing, thereby enhancing the comfort and usability of mobile monitoring. A recent review has been written by Chi et al. (Chi 2010) concerning the novel systems in the area of dry-contact and noncontact biopotential electrodes. LifeShirt from Vivometrics Inc. (Grossmann 2004) and SmartShirt from Sensatex Inc. (Sensatex) are examples of commercialized systems for wearable ECG monitoring. Another commercialized system is provided by Zephyr Technology Corp.; this measures vital signs, including ECG, breathing rate, skin temperature, activity, and posture (Zephyr). Several other e-textile technologies have been introduced that embed sensors in garments (Marculescu 2002; DeVaul 2003; Martin 2003).

The Lifeguard project at Stanford University is a physiological monitoring system that includes physiological sensors connected to a wearable device with a built-in accelerometer (NASA). The HealthGear project uses a similar architecture, transmitting medical data to a user's cellular phone (Flores-Mangas 2005). The CustoMed project at UCLA provides a plug-and-play approach to medical sensing in which hardware and software combinations can be customized to the needs of individual patients (Jafari 2005). Moreover, AMON is a EU IST funded wearable medical monitoring and alert system targeting high-risk cardiac/respiratory patients, and includes measurement of SpO_2, one lead ECG, blood pressure, acceleration, and temperature (Anliker 2004). In our department, we have also developed textile-based wearable systems. We have studied the suitability of silver yarn electrodes for mobile ECG recording (Puurtinen 2006; Cömert 2008), and developed wearable electromyographic (EMG) and electro-oculographic (EOG) measurement systems for psychophysiological applications and computer-human interaction (Nöjd 2005; Puurtinen 2005[a]; Puurtinen 2005[b]; Vehkaoja 2005[a]; Vehkaoja 2005[b]).

Real-time signal analysis

The availability and low cost of personal computers and workstations has allowed for the development of automated signal processing algorithms. Thus, current wearable devices are able to provide more sophisticated signal processing tools and even real-time signal analysis. Recently, Leijdekkers et al. reported the trial results of a cardiac rhythm management system using smart phones and wireless ECG sensors (Leijdekkers 2009). Further, Finnish CorusFit Oy and Tampere University of Technology have developed a system for wearable ECG monitoring during group training, which can be utilized for the rehabilitation of cardiac patients (CorusFit ; Vehkaoja 2008). Their goal is to help patients—both those already diagnosed with CAD and those at high risk—to achieve a permanent lifestyle change. The electrode montage used in their wearable ECG application is similar to lead CM5, which is also studied in this thesis.

Implantable devices

Sensor technology for implantable applications has also been developed to enable measurement of biosignals inside the human body (Riistama 2007; Väisänen 2010). Further, implantable cardiac event monitors have also proved effective in detecting cardiac arrhythmias (Benditt 2003; Burke 2003; Farwell 2004; Sarkar 2008) and acute ischemia (Song 2004). One publication on the CardioAlarm system concluded that a 4 cm square subcutaneous sensor with electrodes at its corners can reliably monitor cardiac activity and accurately detect the occurrence of cardiac arrest (Arzbaecher 2006). The IED (4 cm) and electrode location (near the standard electrodes V3-V4) used in the CardioAlarm trials is similar to that studied in this thesis. The commercial

implantable cardiac event monitors include those of Reveal by Medtronic (Medtronic) and Confirm by St. Jude Medical (StJudeMedical), which provide monitoring for up to 3 years. They continuously monitor heart rhythms and can record an ECG at the time of, e.g., fainting; moreover, they may help to confirm or rule out life-threatening arrhythmias.

Finally, it is worth mentioning that there are also emerging methods of monitoring ECG signals, such as capacitive sensors. The capacitive method is based on inductive coupling, and such devices have been reported by, e.g., Ueno et al. (Ueno 2007) and Lekkala et al. (Lekkala 2010). The quality of the capacitively measured signals shows that this method has potential for a new kind of measurement interface in wearable and body sensor applications where a near field reading technique can be used.

3.2 Modeling in ECG lead development

Human tissues have different electrical properties and the whole human body acts as a volume conductor. Electrical currents form one important means of cellular function and signal transfer in the human body, and the signals arising from bioelectrical sources such as the heart, brain, and skeletal muscle can be measured on the body surface. The fields generated by these sources can also be studied using bioelectrical models. To model and solve bioelectric field problems, either the forward or the inverse problem can be used. The forward problem is solved by starting from a given electrical source and conductor, and calculating the potentials at the electrodes. In contrast, the inverse problem means that the field and the conductor are known, but the source is unknown (Malmivuo 1995). The research in this thesis was conducted by using the inverse problem.

Since investigation of the performance of new electrode systems may be tedious if numerous clinical trials are needed, modeling tools provide new means of predicting the behavior of physiological signals. The behavior of a biological system can be simulated or formulated to a certain degree by models that approximate certain anatomical and physiological features, and models have been utilized in a number of biomedical applications. In electrocardiology, one of the earliest ECG models was the homogeneous thorax model used by Frank, the founder of the current vector ECG system (Frank 1954; Frank 1956). Later models have been especially valuable in applications where in vivo measurements are not always possible, such as in developing implantable devices. Thus, models have been used, e.g., for implantable defibrillator electrode comparison (Gale 1994), and for evaluation and optimization of defibrillation fields (Mohammed 1993; Panescu 1995).

One important aspect of ECG is understanding what area of the model a certain lead measures. This can, for example, be achieved by studying the measurement sensitivity

distribution using the lead field. The formulation of lead field theory was originally introduced by Richard McFee and Franklin D. Johnston (McFee 1953; McFee 1954[a]; McFee 1954[b]), and it is further described in the Methods chapter. To mention a few applications, the lead field theory has been utilized in developing so-called aimed leads to detect local myocardial activation (Hyttinen 1994), for developing impedance cardiography (Kauppinen 1999; Kauppinen 2000), and for designing implantable ECG monitors (Väisänen 2006; Väisänen 2006). Apart from ECG, the lead field method has been used in analyzing the spatial resolution or sensitivity distributions of EEG (Väisänen 2008; Wendel 2010). In addition, we have used the lead field method to model the measuring sensitivity of facial EMG leads (Puurtinen 2005[b]).

3.3 Body surface potential map data

Body surface potential mapping (BSPM) is a technique used to capture high-resolution recordings of the heart's activities by measuring the ECG signal from several electrodes on the subject's chest (Figure 2). Compared to the traditional 12-lead system, BSPM provides higher spatial accuracy and amount of information for use in different applications (Nadeau 1995; Kornreich 1997). Hence, BSPMs contain diagnostic information not present in conventional lead systems and offer extensive material for analyzing different lead configurations. Kornreich et al. have utilized BSPM material to, e.g., identify the best ECG leads for diagnosing acute myocardial ischemia or LVH (Kornreich 1988; Kornreich 1989; Kornreich 1998). Regarding wearable systems, Finlay et al. investigated the issues of electrode placement in smart clothing (Finlay 2008). They analyzed a BSPM set of 192 unipolar leads, and based on their experiments, recommended using anterior and precordial areas.

Regarding bipolar leads, BSPM has been utilized for determining the optimal region for a small implantable monitor (Burke 2003; Song 2004; Arzbaecher 2006), and it was found that closely spaced bipolar precordial leads can be used for automatic detection of acute ischemia, ventricular tachycardia (VT), or ventricular fibrillation (VF). Regarding surface ECG, Tomašić et al. recently introduced a multivariate linear regression–based synthesis of 12-lead ECG from three closely spaced bipolar leads (Tomašić 2010). In a further publication by Trobec et al., the researchers concluded that just three bipolar leads suffice for reliable synthesis of the 12-lead ECG (Trobec 2011).

Nevertheless, the problem of identifying the most appropriate site for a small wireless bipolar one-lead ECG device remains unsolved. This information would be useful for new emerging wireless, wearable, and handheld surface ECG devices. High-resolution BSPM recordings offer a valuable tool for testing multiple bipolar leads.

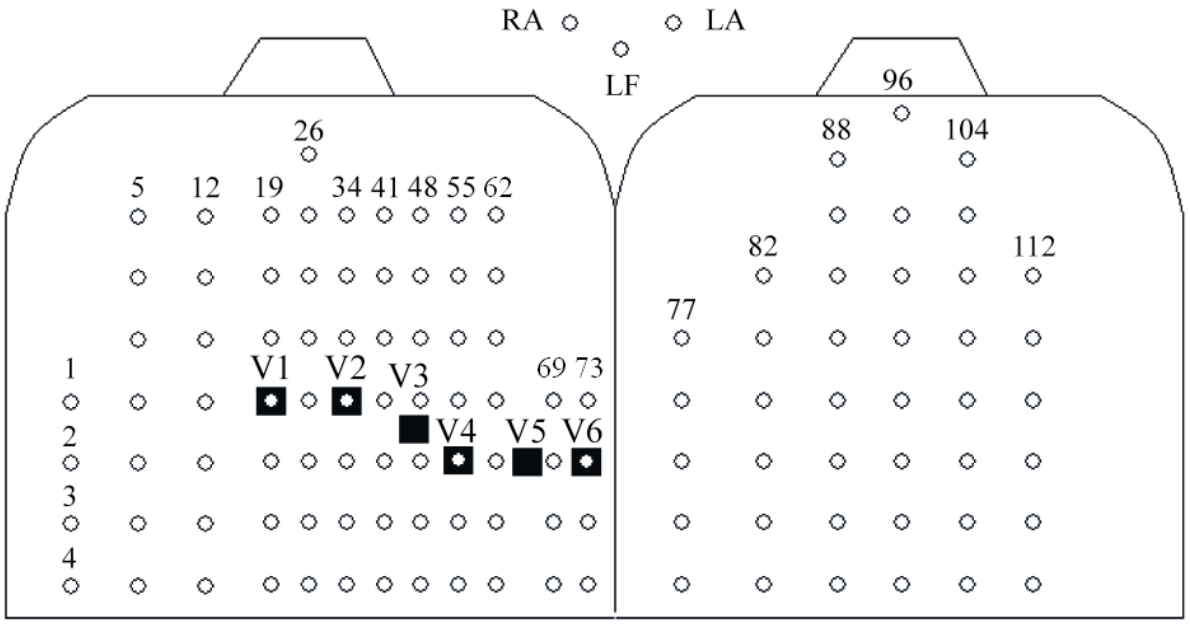

Figure 2. The 120 body surface potential map (BSPM) electrode locations in the Dalhousie lead system (Hoekema 1999). The black squares illustrate the location of the chest electrodes of the standard 12-lead system leads V1-V6. RA: right arm, LA: left arm, LF: left foot. [I]

3.4 Left ventricular hypertrophy

Left ventricular hypertrophy (LVH) is associated with the risk of cardiovascular events, including ischemic heart disease, vascular disease, and sudden death (Casale 1986; Levy 1990; Koren 1991; Schillaci 2000). The importance of diagnosing LVH has increased in recent years with the recognition that hypertrophy can be reversed and the adverse clinical outcomes delayed with therapy (Mathew 2001; Okin 2003). LVH can be diagnosed with ECG, and the commonly used LVH-ECG criteria are based on 12-lead system electrode locations and QRS voltages. Many voltage criteria have been introduced over the years, most notably by Sokolow and Lyon (Sokolow&Lyon 1949), who introduced the criterion based on the sum of S_{V1} (S amplitude in lead V1) and R_{V5} or R_{V6} (R amplitude in lead V5 or V6) in 1949. Other criteria include the sum of S_{V3} and R_{aVL}, referred to as the Cornell voltage (Casale 1985), and the point score of Romhilt and Estes (Romhilt 1968). More recently, increasingly complex criteria have been developed, such as the computation of QRS area, composite use of several criteria, and incorporating multiple electrocardiographic and nonelectrocardiographic factors (Schillaci 1994; Norman 1995; Okin 1995; Okin 1996; Rautaharju 1996). Thus, the LVH-ECG criteria have evolved over the years, and the recent AHA Recommendations for the Standardization and Interpretation of the Electrocardiogram comprises recommendations for the standardization of LVH interpretation (Hancock 2009).

LVH diagnostics has also evolved through BSPM data. Kornreich et al. identified the best unipolar leads for diagnosing LVH by statistical analysis of BSPMs (Kornreich 1988; Kornreich 1989). They used time-normalized P, PR, QRS, and ST-T waveforms and the duration of these waveforms. The best five results were obtained from BSPM unipolar leads 24 and 38 at the lower precordium, leads 73 and 80 on the left side, and lead 113 on the back (see Figure 2 for electrode locations). Further, Oikarinen et al. assessed the capability of BSPM unipolar leads' QRS area in LVH diagnosis (Oikarinen 2004). As best locations, they identified BSPM unipolar leads 9 and 10 on the lower right precordium, leads 7 and 13 on the upper right precordium, and lead 78 on the left lower flank area (see Figure 2 for electrode locations). In addition, Malmqvist et al. studied the influence of using modified limb electrodes (limb leads placed on the abdomen instead of the extremities) on various LVH criteria (Malmqvist 2000). They concluded that ECGs registered with modified limb electrode positions can be used to detect LVH with traditional ECG criteria, but changes in the limb leads are considerable and influence the sensitivities.

The above-mentioned studies concentrate on unipolar leads or modified limb electrodes in the diagnosis of LVH. To our knowledge, the performance of bipolar leads with a short IED in LVH diagnosis has not been previously reported. Thus, one of the aims of this thesis (publication [III]) was to study the performance of a closely spaced bipolar lead in differentiating LVH subjects from normal subjects.

3.5 Exercise test and coronary artery disease

The exercise test is a diagnostic tool for evaluating the cardiovascular responses to physical exercise in a controlled clinical environment. The most common methods of exercise testing are the bicycle ergometer and the treadmill (Fletcher 1995; Froelicher 2000). During the test, progressive workloads are used and patients' ECG, blood pressure, respiration, and symptoms are monitored.

In exercise ECG, the commonly used electrode placement is the Mason-Likar modification of the 12-lead system (Figure 3). In Mason-Likar, the conventional limb electrodes are placed at the base of the limbs instead of the extremities. Figure 3 also illustrates two additional leads, V4R and CM5, which can be used in exercise ECG. V4R is a unipolar lead with the WCT as the reference, and CM5 is a bipolar lead recorded between the manubrium (electrode M in Figure 2) and the location of the chest electrode of standard lead V5.

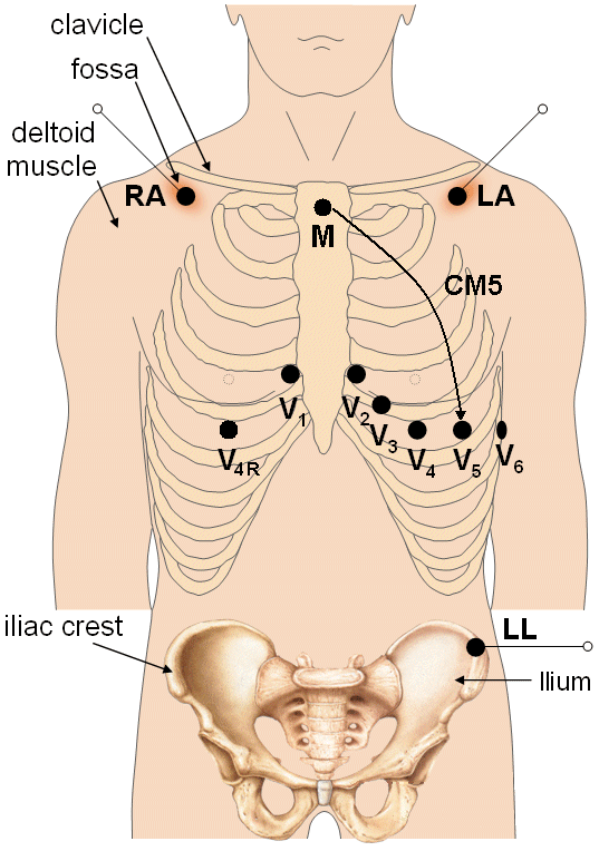

Figure 3. Mason-Likar modification of the standard 12-lead system electrode placement for exercise test and additional electrodes V4R and M for leads V4R and CM5. Modified from (Malmivuo 1995).

Controlled exercise testing is an important diagnostic tool because it can bring out symptoms and characteristic changes on the ECG that become apparent only during physical exercise. Thus, the exercise test is generally used in the diagnosis of coronary artery disease. CAD is one of the main cardiovascular diseases, and is caused by atherosclerosis, which gradually reduces the blood flow capacity of the coronary arteries. Reduced blood flow may lead to ischemia of the heart muscle, and the first symptoms, such as chest pain, often occur during physical stress. The procedure for diagnosing CAD usually starts from detected symptoms, and the patient can be further examined with the exercise test.

One of the main goals of the exercise test is to reveal clinically significant and symptomatic stenosis in coronary arteries. In the case of positive indications, coronary angiography can be conducted for further localization and measurement of the degree of the stenosis. The coronary arteries may also be examined by using computed tomography (CT) or single-photon emission computed tomography (SPECT). Still, the exercise test is an important diagnostic modality for the evaluation and diagnosis of cardiac conditions because it is noninvasive and has an independent prognostic value.

It gives information on whether the patient has symptoms during exercise, and on which workload or heart rate the symptoms are induced.

All in all, the exercise test elicits changes in HR, blood pressure, respiration, and perceived level of exercise that provide information on patients' cardiovascular and respiratory performance. In addition to these changes, exercise induces alterations in the ECG waveform. Normal changes include shortening of the PR, QRS, and QT intervals, an increase in the P-wave magnitude, and small changes in Q-waves (MacFarlane 1989; Simoons 1989; Jain 1995; Froelicher 2000). The most prominent abnormal change in ECG during exercise is ST-segment deviation, which is associated with exercise-induced ischemia in patients with significant coronary obstruction (Stern 2002). The amount (mm or mV) of ST-segment deviation is generally measured 60 or 80 ms after the J-point (the junction between the QRS and the ST-segment), and usually a positive test criterion of 1.0 mm (mV) ST-depression is used to indicate ischemia.

One disadvantage of exercise testing is that it has limited sensitivity and specificity. A meta-analysis of 147 studies reported that exercise-induced ST-segment alterations identified coronary artery disease with a mean sensitivity of 68±16% and a mean specificity of 77±17% (Gianrossi 1989). The use of right precordial leads along with the standard six precordial leads has been reported to greatly improve the sensitivity of exercise testing for the diagnosis of CAD (Michaelides 1999). In addition, other studies that used recordings from the V4R lead during exercise testing have reported a small improvement in the detection of right CAD (Braat 1985; Chouhan 1989). However, other studies suggest that the application of right precordial leads does not improve the accuracy of the exercise ECG, even though it may contribute to the detection of ischemia perfused by the right coronary artery (Wierzbowska 2002; Ueshima 2004). Thus, there are controversial results as to whether additional leads improve the performance of exercise ECG. It has been reported that the exercise ECG leads have dissimilar diagnostic properties in the detection of CAD (Viik 2000), so it would be interesting to study the additional value of leads V4R and CM5 further. The benefit of lead CM5 is that it can be utilized in wireless applications, as it does not use the WCT as reference. In the Finnish Cardiovascular Study (FINCAVAS), leads V4R and CM5 are included in the exercise ECG protocol in addition to the standard 12-lead system (Nieminen 2006). Thus, it offers a valuable database for studying the performance of these additional leads in the detection of CAD.

4. MATERIALS AND METHODS

This thesis adopts three different approaches to test new bipolar ECG lead configurations: modeling, clinical BSPM data, and exercise ECG data. Section 4.1 presents the modeling methods in the analysis of the measurement sensitivity of ECG leads, Section 4.2 presents the clinical BSPM database that was utilized to optimize bipolar electrode locations for normal subjects and for subjects with LVH, and Section 4.3 presents the exercise ECG data that was utilized for evaluating additional ECG leads in CAD detection. Finally, Section 4.4 presents the statistical methods applied.

4.1 Modeling of the measurement sensitivity of ECG

4.1.1 Thorax models

The models used in publication [I] were three-dimensional (3D) finite difference method (FDM) thorax models. FDM models are usually constructed from biomedical images, such as those obtained by magnetic resonance (MR) or CT. The modeled domain is subdivided or discretized into a grid of rectangular voxels, each with a resistivity defined by the corresponding tissue. The corners of a voxel form nodes and the conducting volume between adjacent nodes is replaced by an equivalent resistor. In this resistor network, most bioelectric field problems can be formulated in terms of either the Poisson or the Laplace equation, and an iterative method is used to approximate the solution at each node.

In this thesis, two realistic but passive FDM models were used (the activation of the heart was not modeled), specifically a 3D model based on the visible human man (VHM) project and a 3D model based on MR images presenting the anatomy during diastole (Puurtinen 1999; Puurtinen 2001; Takano 2002). We hereafter refer to these models as Model 1 and Model 2, respectively. The anatomy of Model 1 was based on

a particularly accurate source of anatomical data, the U.S. National Library of Medicine's (NLM's) VHM data (NLM ; Ackerman 1991; Spitzer 1996; Spitzer 1997) and extracted from a full thorax model by Kauppinen and associates (Kauppinen 1998). This model represented segmented transverse slice images of a male cadaver thorax, and included all visible details and 36 tissue types.

The anatomy of Model 2 was derived from a set of MR images provided by Professor Robert Patterson, University of Minnesota. The image data comprised 70 transverse slices presenting the anatomy during diastole. Altogether, this model included 26 distinct tissue types, including, e.g., intracavitary blood, the pericardium, major vessels, lungs, subcutaneous muscles and fat, bone, and some internal organs (liver, spleen). The main inhomogeneities included in the models and their resistivity values are listed in Table 1 (Puurtinen 1999; Hyttinen 2000; Takano 2002). Models 1 and 2 are illustrated in Figure 4 with the appearance of the heart. For the current study, the resolution of both models was adapted so as to provide a more accurate presentation of the anatomy in the left anterior thoracic area, where the cardiac sources are located. In this area, the element size was 3.3 mm x 3.3 mm x 4 mm in Model 1 and 3 mm x 3 mm x 5 mm in Model 2, increasing toward the back of the thorax and to the right side. The resolution of the back and right sides of the thorax models were made coarser in order to enable calculations on the otherwise heavy 3D models. Model 1 included a total of 258,442 nodes and Model 2 a total of 253,468 nodes.

Table 1. The main inhomogeneities included in the models and their resistivity values.

Inhomogeneity	**Resistivity (Ω cm)**
Bone	2,000
Lungs	1,325
Subcutaneous fat	2,000
Skeletal muscle	400
Liver	600
Stomach	400
Heart fat	2,000
Heart muscle	450
Blood masses*	150
Other tissues and organs	460

*Including intracardiac blood masses, great arteries, and veins

a) b)

Figure 4. The realistic 3D thorax models: (a) model based on the visible human man project; (b) model based on magnetic resonance images presenting the anatomy during diastole [I].

4.1.2 Modeling calculations

In study the properties of ECG electrode configurations, the lead field theory provides a means of estimating the measurement sensitivity and thus the signal strength. The model calculations in publication [I] were based on the lead field and reciprocity theorems. The relationship between the measured signal V_{LE} in the lead and the cardiac current sources $\overline{J}^i$ in the volume conductor can be formulated as follows:

$$V_{LE} = \int \frac{1}{\sigma} \overline{J}_{LE} \bullet \overline{J}^i dv \qquad (1),$$

where $\overline{J}_{LE}$ is the lead field and σ is the conductivity of the volume conductor (Malmivuo 1995). Thus, if the lead field and the properties of the volume conductor are known, the strength of the measured signal V_{LE} can be estimated. The problem is simplified by assuming a case of uniform source distribution; thus, the lead sensitivity can be expressed as an average of the lead vectors J_{LE}. The reciprocity theorem states that the location of the source (equivalent dipoles in the heart muscle) and the detector (electrodes) can be interchanged without any change in the signal amplitudes (Malmivuo 1995). We therefore applied a reciprocal current to the measuring electrodes located on the model, and calculated the resulting lead field in the heart muscle. To obtain the average measuring sensitivity for the whole source (heart muscle) area, we calculated the average magnitude of the resultant lead field vectors in the heart muscle. This represented the leads, i.e., the electrodes' sensitivity to measuring the electric source of the heart. Then, to evaluate whether the modeling results represented the actual clinical data, we compared the modeled measuring

sensitivity with the signal strength obtained from the clinical BSPM data. A total of 117 unipolar and 42 bipolar leads were studied. The methods are further described in publication [I].

For the modeling calculation, we utilized bioelectric field software that was originally developed by Walker at the University of Tasmania (Walker 1985; Walker 1987). The software has been further developed by Hyttinen and Kauppinen et al. (Hyttinen 1994; Kauppinen 1999), and the version used in publication [I] of this thesis was developed by Takano (Takano 2002).

4.2 Body surface potential map data

4.2.1 BSPM material for normal and LVH subjects

In this thesis, a BSPM database was utilized for three purposes: (a) validating the modeling results [I], (b) defining optimal locations for a small bipolar ECG device [II], and (c) defining optimal locations for a small bipolar ECG device to differentiate subjects with LVH from normal subjects [III]. The BSPM database was kindly provided by Professor Friedrich Kornreich, Vrije Universiteit Brussel, Belgium. These BSPM data consisted of 120-lead ECGs acquired from 236 normal subjects and 305 subjects with LVH. The presence of LVH was diagnosed from ECG-independent information, specifically from echocardiography, cardiac catheterization with coronary angiography and ventriculography, radionuclide angiography, chest radiographs, or cardiac surgery. The LVH population was further subdivided into 116 pure left-sided valvular disease or sustained hypertension (150/90 mmHg or higher) and 189 complex LVH patients with various cardiac conditions frequently associated with LVH (Kornreich 1989; Kornreich 1993).

The electrode system comprised three unipolar limb leads (RA: right arm, LA: left arm; LF: left foot) and 117 body surface unipolar leads. The 117 body surface electrode positions were defined with a grid of 9 rows and 18 columns. This electrode system is referred to by Hoekema as the Dalhousie lead system (Hoekema 1999). The electrode locations are illustrated above in Figure 2. These BSPM ECG data contained preprocessed and parameterized unipolar signals recorded with WCT as reference. The data sample from each subject comprised ensemble averages of ECG voltages at 52 time points set in a time-normalized P-to-T complex waveform (Kornreich 1989).

4.2.2 Electrode locations

The unipolar leads studied in this thesis corresponded to those of the original BSPM data. The bipolar electrode locations were chosen in the left precordial area, as the ECG signal arises there. The precordial area and especially the locations close to the chest electrodes of the standard leads V1-V6 were expected to give the best signal strength, as well as information on interindividual variability. As the BSPM data included only unipolar leads, the bipolar leads were formed by subtracting the signals of selected unipolar leads from one another.

In publication [I], the BSPM data were utilized to validate the results of the modeling study. A total of 117 unipolar and 42 bipolar leads (14 horizontal, 28 vertical) were studied (Figure 5 (a)). The 117 unipolar locations were those in the original BSPM data, and the bipolar electrode locations were chosen so that they would be close to the chest electrodes of the standard leads V1-V6. As illustrated in Figure 5 (a), the bipolar leads represented different IEDs; in this way, we could also evaluate the effect of IED on signal strength.

In publication [II], the aim was to optimize the location and direction of a small plaster-like ECG sensor; thus, only bipolar leads with short IEDs were analyzed. The distance was approximately 5 cm vertically, 6 cm horizontally, and 6 cm diagonally, depending on the person's size. The rationale for this electrode spacing was that the original BSPM data directly supported this spacing, and that it represents a possible size for a wearable or implantable ECG device. A total of 42 vertical, 35 horizontal, and 36 diagonal bipolar leads were analyzed to find the lead locations that would maximize the ECG signal strength within normal subjects (Figure 5 (b)).

In publication [III], the aim was to test the performance of small ECG sensors in detecting LVH. We studied similar bipolar lead configurations to those in publication [II], and added one diagonal lead direction. An additional lead direction was included because LVH is known to shift the QRS axis (Wagner 2007), and we considered that new electrode directions could give additional information. The formed bipolar leads on the anterior thorax included 36 vertical, 30 horizontal, 36 diagonal sloping downwards left (dL), and 30 diagonal sloping downwards right (dR) leads (Figure 6). These bipolar leads were analyzed to find those that best differentiated LVH subjects from normal subjects. The electrode numbering was adjusted in publication [III] for practical reasons; electrode 1 in publication [III] corresponded to electrode 19 in the original BSPM data.

In all three publications [I-III], the bipolar signals were obtained by subtracting the unipolar BSPM signals of selected electrode pairs from each other using a Matlab script. In publication [I], the IED varied, as illustrated in Figure 5 (a). In publications [II] and [III], the IEDs of the bipolar leads were 5–6 cm.

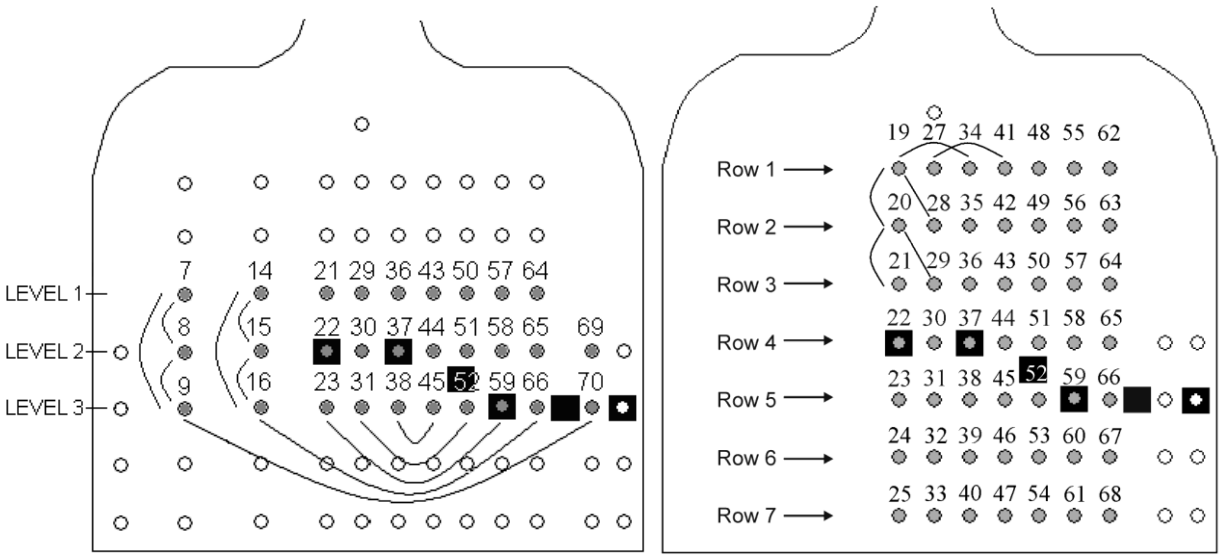

(a) (b)

Figure 5. Location of bipolar leads analyzed in a) publication [I], b) publication [II]. Analyzed electrodes are numbered and colored in grey. Black squares denote the location of the chest electrodes of leads V1-V6 in standard 12-lead ECG [I, II].

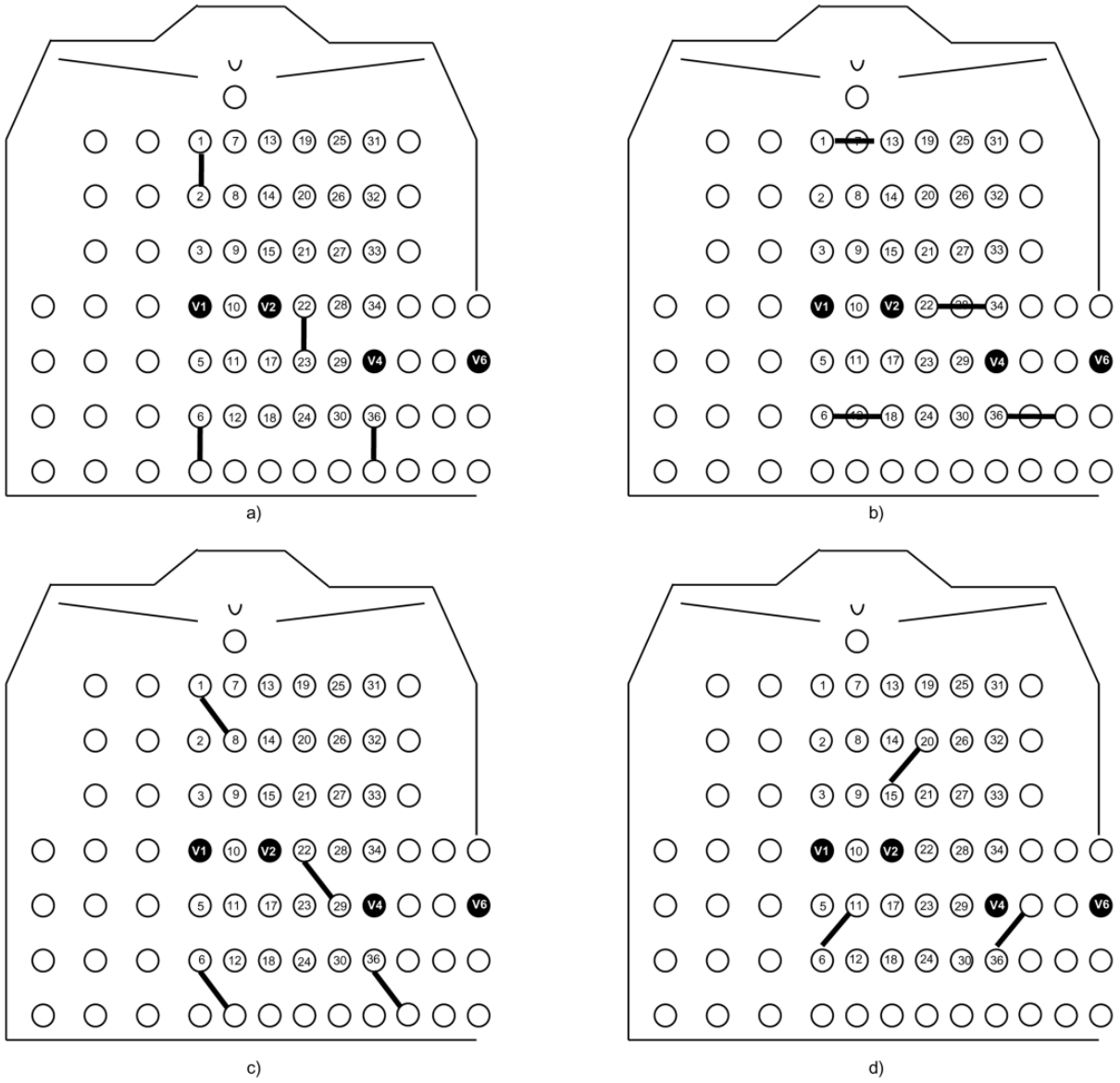

Figure 6. Location of bipolar leads analyzed in publication [III]. Leads oriented (a) vertically, (b) horizontally, (c) diagonally sloping downwards left (dL), and (d) diagonally sloping downwards right (dR). Black circles denote the location of the chest electrodes of standard 12-lead ECG precordial leads [III].

4.2.3 Signal analysis

In this thesis, signal analysis was utilized to detect and calculate the average P-wave and QRS complex amplitudes from the 120-lead BSPM ECG signals recorded from different persons. These amplitudes were chosen to represent the lead's signal strength.

The ECG signal analysis for publications [I-III] was conducted with Matlab. To validate the modeling method in publication [I], we compared the modeled measuring

sensitivity with the signal strength obtained from corresponding electrodes in BSPM. The average QRS amplitude was chosen to represent the ECG signal strength in BSPM data. We calculated the peak-to-peak value (the sum of the absolute values of negative and positive amplitudes) of the QRS complex to give the full amplitude during ventricular activation, and calculated the average QRS amplitude within all 236 normal patients.

To optimize the location of a small bipolar lead within normal subjects in publication [II], both QRS complex and P-wave amplitudes were derived from the 120 bipolar lead signals. The QRS amplitude was calculated as in publication [I]. Similarly, the P-wave amplitude was calculated—with the baseline adjusted to the TP (the plateau phase between T wave and P-wave) segment—to give the amplitude during atrial activation. QRS and P amplitudes were defined for each subject and the average and standard deviation were determined. The P-wave was targeted, as it is usually one of the smallest of the diagnosed parameters in the ECG, and thus is the first to disappear under noise. For reference, we compared the signal amplitudes obtained from bipolar leads to noise levels of 15 μV and 60 μV; these values represent a fairly low and a rather high noise level in normal ECG measurements (Fernandez 2000; Huigen 2002). Noise values were taken from the literature, as noise could not be analyzed from readily parameterized and preprocessed BSPM data.

In publication [III], the BSPM ECG signals were utilized to evaluate the performance of new small bipolar leads in LVH diagnosis. We studied whether small bipolar leads are able to discriminate subjects with LVH from normal subjects based on QRS amplitude. Thus, the QRS amplitude was defined for each subject and each lead. For reference, the analysis was also conducted for standard leads V1, V2, and V4, which were available in the BSPM database. The subjects in the ECG database were divided into two groups: normal (n=236) and LVH (n=116). The performance of the bipolar leads in differentiating LVH subjects from normal subjects was further assessed with receiver operating characteristic (ROC) analysis, which is presented in Section 4.4.

4.3 Exercise ECG data for CAD

4.3.1 FINCAVAS database

In publication [IV], the approach was slightly different from the other publications. While publications [I]-[III] analyzed the performance of new small bipolar leads for wireless applications utilizing BSPM data, publication [IV] analyzed the value of leads V4R and CM5 in CAD detection utilizing exercise ECG data. The reasoning for this was that CM5 is also a bipolar lead located on the chest (see Figure 3), and it could be used in wireless and portable applications. CM5 could be especially useful in wearable t-shirt ECG systems, such as that developed by the Finnish CorusFit Oy and Tampere

University of Technology. Their solution includes wearable ECG monitoring during group training, and their rehabilitation programs and methods can be applied among people at risk for or already diagnosed with CAD (CorusFit ; Vehkaoja 2008). One of the leads measured in CorusFit WiEKG and SensorWear is similar to lead CM5. Thus, it is interesting to evaluate the performance of this lead using an exercise ECG database.

The exercise ECG database used in publication [IV] was a previously documented FINCAVAS database (Nieminen 2006). The purpose of FINCAVAS is to construct a risk profile of individuals at high risk of cardiovascular diseases, events, and death. The FINCAVAS has an extensive set of data on patient history, genetic variation, cardiovascular parameters, ECG markers, and follow-up data on clinical events, hospitalizations, and deaths. Between October 2001 and December 2008, all patients scheduled for a standardized clinical exercise test at Tampere University Hospital, Tampere, Finland and willing to participate in the study were recruited. About 20% of the patients had also undergone coronary angiography within 6 months of exercise testing. The study protocol in FINCAVAS was approved by the Ethical Committee of the Hospital District of Pirkanmaa, Finland, and all patients gave informed consent prior to the interview and measurements, as stipulated in the Declaration of Helsinki.

The published FINCAVAS database comprises information on 2,212 patients examined between October 2001 and December 2004 (Nieminen 2006). For publication [IV], patients with an exercise test shorter than 4 min, left or right bundle branch block, LVH, type 1 diabetes, and those taking digitalis medications were excluded. In addition, patients who underwent coronary artery bypass surgery between the exercise test and angiography and patients with a recent ($\leq$ 8 weeks) myocardial infarction were also excluded.

For publication [IV], the patients were further divided into the following three subgroups based on angiography and clinical history.

Angiographically proven CAD (CAD). This group consisted of patients who had $\geq$ 50% luminal diameter narrowing in at least one major epicardial coronary artery or side branch. The CAD group comprised 255 patients, of which 201 were men and 54 women.

No CAD by angiography (NoCAD). This group consisted of patients who had no evidence of CAD either in the major coronary arteries or in the side branches. The NoCAD group comprised 126 patients, of which 62 were men and 64 women.

Low likelihood of CAD (LLC). This group consisted of patients who did not undergo coronary angiography but had no clinical signs of cardiac diseases. To be included in this subgroup, the patients needed to have no history of cardiac disease and no cardiac medication (short- or long-acting nitrates, β blockers, digitalis, diuretics, calcium [Ca] channel blockers, angiotensin converting enzyme [ACE] inhibitors, or angiotensin 2 antagonists). In addition, the patients did not have angina pectoris during exercise, and the probability of CAD was considered to be low according to the supervising physician. The LLC group comprised 198 patients, of which 117 were men and 81 women.

4.3.2 Exercise test protocol

Prior to the exercise stress test, the subject lay down in a supine position for 10 min, and the resting ECG was digitally recorded. The exercise test was performed using a bicycle ergometer, and the ECG lead system was the Mason-Likar (Mason 1966) modification of the standard 12-lead system and an additional two electrodes for recording leads V4R and CM5 (Nieminen 2006). During the test, HR was continuously registered with ECG; the systolic (SAP) and diastolic (DAP) arterial pressures were measured with a brachial cuff every 2 min.

The continuous ECG was recorded at 500 Hz with the CardioSoft exercise ECG system (Version 4.14, GE Healthcare, Freiburg, Germany) and analyzed by Modified CASE software (GE Healthcare, Freiburg, Germany). All ECG parameters recorded during the exercise were determined at 14 points in time: before exercise, seven times during the exercise (start, 2 min, 4 min, 6 min, 8 min, 10 min, and maximal load), and six times during recovery after the exercise at the end of each minute up to 6 min.

4.3.3 ST-segment analysis

We used ST-segment depression as a parameter to evaluate whether the application of leads V4R and CM5 enhanced the diagnostic performance of the exercise ECG in the detection of CAD. The variable used in the ROC analysis of publication [IV] was ST-segment depression at peak exercise. ST-segment depression was determined from the 12-lead system and from the additional leads V4R and CM5. Leads V1 and aVL were excluded from the study. Leads aVR and V4R were inverted because of the rightward direction of the leads. When studying lead sets, the maximum value over the studied leads was used as the classifier for the variable. ST-segment amplitudes were measured to the nearest 10 μV at a point 60 ms after the J-point. The traditional positive test criterion for ST-segment depression was used ($\leq$ -0.10 mV ST-segment value, i.e., $\geq$ 1.0 mm ST depression). Angiography was employed as a reference method; this is considered to be the ultimate diagnostic method for CAD because it directly measures the degree of stenosis in the coronary vessels.

4.4 Statistical analysis

The statistical analysis was conducted with Matlab for publications [I] and [II], and with SPSS 16.0 for publications [III] and [IV].

4.4.1 Traditional statistical methods

To assess the relationship between the modeled measuring sensitivity and the signal strength obtained from actual ECG data in publication [I], we conducted a linear correlation analysis with a least-squares fit to calculate the Pearson's linear correlation coefficient. The correlation coefficient indicates to what extent the datasets are linearly associated (Draper 1998).

In publication [II], one aim was to define which electrode location provides a strong and reliable signal independent from the subject. For this, the average and standard deviation (SD) of P-wave and QRS amplitudes were calculated. Standard deviation shows the extent to which the data samples differ from the average value (Dunn 1974). One SD away from the mean accounts for around 68% of the values, and two SDs away account for around 95%, assuming that the data is normally distributed. Thus, we used the SD to describe how reliable the recording site was within different individuals.

In publications [III] and [IV], sensitivity and specificity were used as parameters of the diagnostic properties of the leads. Sensitivity is the proportion of true positives that are correctly identified by the test (e.g., the percentage of sick people who are identified as having the condition). Specificity is the proportion of true negatives that are correctly identified by the test (e.g., the percentage of healthy people who are identified as not having the condition) (Altman 1994).

For a general description of the patient group characteristics in publication [IV], the variables were examined by statistical tests. The categorical variables were examined by Pearson's chi square test, and quantitative variables were examined by independent samples *t*-test. The independent samples *t*-test compares the mean scores of two groups on a given normally distributed variable. It can be used to draw conclusions about the means of two populations, and to tell whether or not they are similar. It tests the hypothesis that the difference between the means of two samples is equal to 0 (the null hypothesis). One of the results given by the t-test is the two tailed probability *p*. When this so-called *p*-value is less than the conventional 0.05 or 0.01 (5% or 1% chance of rejecting the null hypothesis when it is true), the null hypothesis is rejected and the conclusion is that the two means do indeed differ significantly (Uhari 2001). The lower the *p*-value, the more statistically significant the result will be.

4.4.2 Receiver operating characteristic analysis

In publications [III] and [IV], the overall diagnostic performance of the studied leads was evaluated using receiver operating characteristic analysis. An ROC curve is a graphical plot of sensitivity vs. (1-specificity) (Figure 7). The perfect classification method would yield a point in the upper left corner of the plot area. This would represent 100% sensitivity (no false negatives) and specificity (no false positives). Again, the diagonal line $x = y$ represents the strategy of random classification. Accordingly, values 1 and 0.5 for the area under the ROC curve represent perfect classification and random classification; respectively. The area under the ROC curve (hereafter referred to as the ROC area) represents the probability that a random pair of patients with and without the condition will be correctly diagnosed (Hanley 1982). The ROC curve includes all values of the selected variable and was plotted using different variables, specifically QRS amplitude and ST depression, in publications [III] and [IV], respectively.

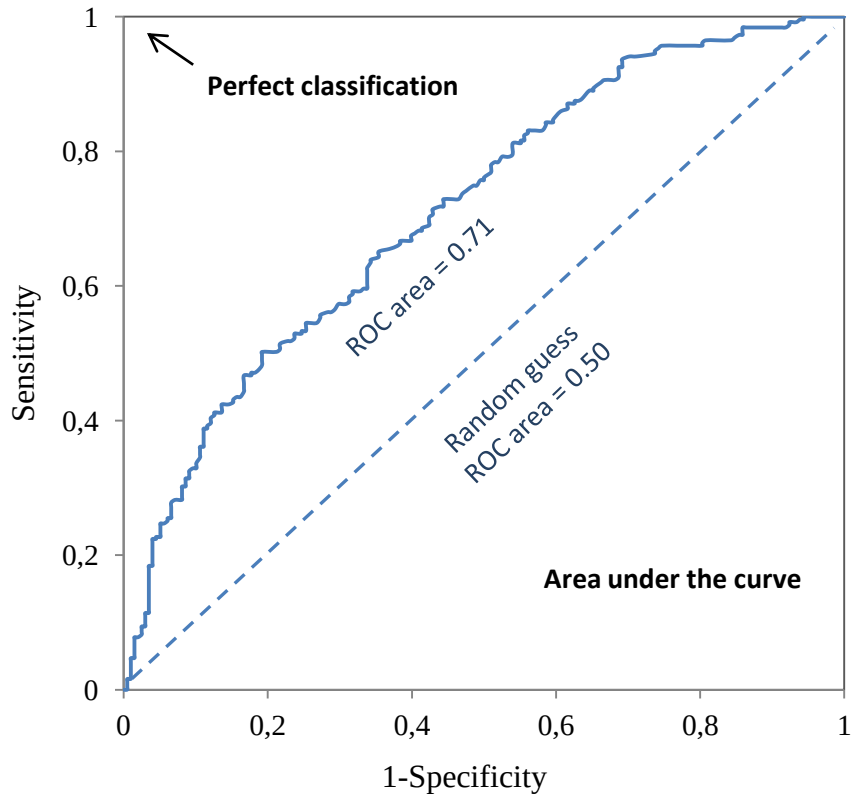

Figure 7. Characteristics of the ROC curve. The diagonal dashed line represents the strategy of random classification (ROC area = 0.5) and the full line represents an example ROC curve with an area of 0.71.

In [III], ROC analysis was used to evaluate the performance of new short-distance bipolar leads in differentiating LVH subjects from normal subjects. The diagnostic variable used in the ROC analysis was the QRS amplitude, i.e., the maximum peak-to-

peak value of the signal during ventricular activation. For further analysis of the signal level in the bipolar leads that provided the highest ROC areas, the average and SD of the QRS amplitudes were calculated for both normal subjects and subjects with LVH.

In [IV], the ROC analysis was used to assess the value of additional leads CM5 and V4R in exercise ECG and CAD diagnostics. In this case, the diagnostic variable in the ROC analysis was ST-segment depression at peak exercise. First, ROC analysis was conducted for individual leads CM5, V4R, and V5. Lead V5 was included as a reference because it has been shown to be capable of detecting most ischemic responses when a positive criterion of 1.0 mm ST depression is used (Tucker 1976; Fox 1984; Miller 1987; London 1988). Second, to evaluate whether the additional lead CM5 or V4R improve the diagnostic performance, ROC analysis was conducted for the following lead sets: standard leads (i.e., the 12-lead system with the exclusion of V1 and aVL); standard leads + CM5; and standard leads + V4R.

5. RESULTS

This chapter presents the main results of publications [I]-[IV]. The discussion related to each section will take place in Chapter 6 in the respective sections.

5.1 Modeling the sensitivity of ECG leads

In [I], we evaluated whether the ECG signal strength can be estimated by modeling the measuring sensitivity with two realistic 3D thorax models (Figure 4). A total of 117 unipolar and 42 bipolar leads were analyzed.

Unipolar leads
The results for 117 unipolar leads are illustrated in Figure 8. The signal strength obtained from clinical BSPM data and the measuring sensitivity obtained with Model 2 from 117 BSPM unipolar leads (see Figure 4 for electrode numbering) are illustrated in Figure 8 (a). The signal strength was plotted as a function of the electrode location/number. It can be observed that the modeled measuring sensitivities corresponded to the actual BSPM signal strength. However, within unipolar leads located on the heart area, such as electrodes 45 to 60, modeling gave higher values than the clinical data. In contrast, among the unipolar leads locating on the left anterior side, such as electrodes 68 to 76, the clinical data gave higher values than the modeling.

The correlation between signal strength obtained from clinical BSPM data (on the *y*-axis) and measuring sensitivity obtained from Model 2 (on the *x*-axis) for the 117 unipolar BSPM torso leads is illustrated in Figure 8 (b). The correlation coefficient between these two datasets was $r = 0.86$ ($n = 117$, $p < 0.05$).

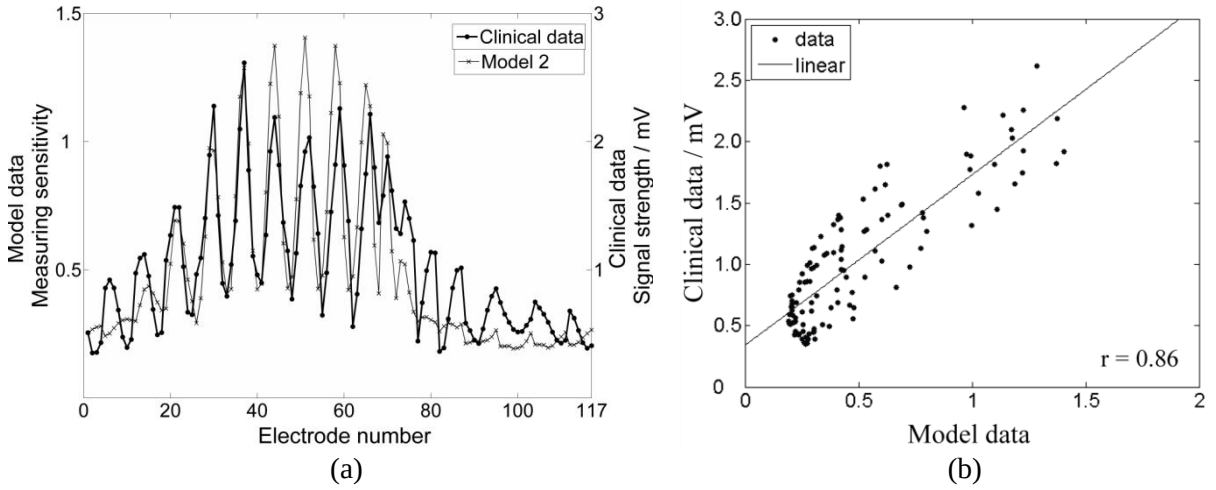

Figure 8. (a) The measuring sensitivity (left y-axis, arbitrary units) obtained from a realistic thorax model (Model 2) and the signal strength (right y-axis) obtained from clinical BSPM ECG data for 117 BSPM unipolar leads. See Figure 4 for electrode numbering. (b) The correlation between the singnal strength from clinical BSPM data (y-axis) and the measuring sensitivity obtained from Model 2 (x-axis, arbitrary units), and the linear regression line. The data points correspond to the same 117 unipolar leads as in (a) [I].

Bipolar leads

The results for the 42 bipolar leads (i.e. electrode pairs) are illustrated in Figure 9 (a) for 14 horizontal and (b) for 28 vertical leads. The three curves in each plot represent the signal strength obtained from clinical BSPM data, the measuring sensitivity obtained from Model 1, and the measuring sensitivity obtained from Model 2.

In Figure 9 (a), the uppermost, middle, and undermost curves illustrate the values for horizontal bipolar leads on *levels 1*, *2*, and *3*, respectively (see Figure 4 (a)). At each level, the leads' IED increases from left to right, being 6 cm in leads 36–43, 37–33, and 38–45. It can be seen that the absolute measuring sensitivity values from both models were different from the clinical data, but the pattern was similar. Thus, the modeled measuring sensitivity corresponded to the relative change in actual signal strength between different leads.

In Figure 9 (b), the uppermost, middle, and undermost curves illustrate the results for vertical bipolar leads between *levels 1* and *2*, *2* and *3*, and *1* and *3*, respectively. The uppermost curve in Figure 9 indicates that in bipolar leads between *levels 1* and *2*, Model 1 corresponded quite well with the results from clinical data. In leads between *levels 1* and *3*, clinical data gave higher values when moving towards the heart area (to the right).

From the linear regression analysis for all 42 bipolar leads in Figure 9, the correlation was $r = 0.62$ between Model 1 and the clinical data, and $r = 0.71$ between Model 2 and the clinical data ($n = 42$, $p < 0.05$ for both).

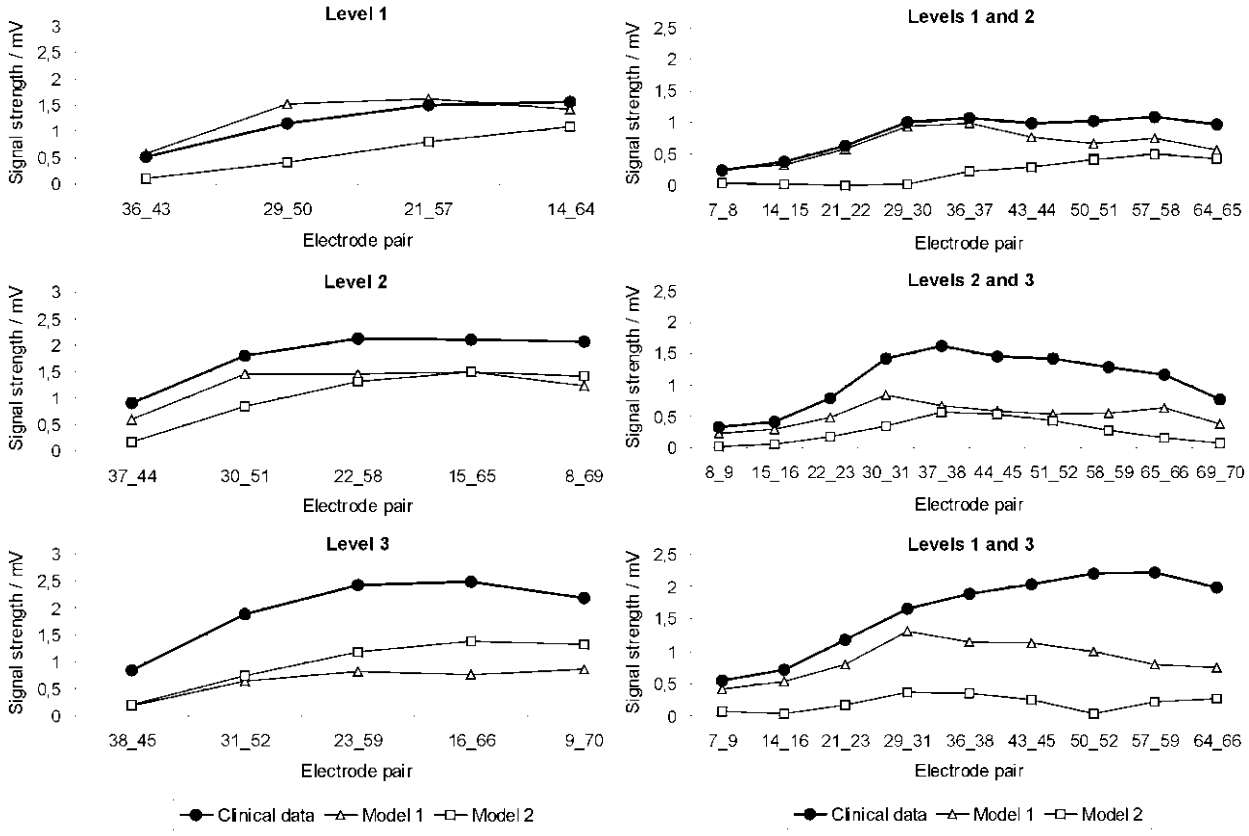

(a) (b)

Figure 9. The signal strength obtained from clinical BSPM data and the measuring sensitivities obtained from Model 1 and Model 2 for (a) horizontal and (b) vertical bipolar leads. The leads were formed from electrode pairs on different levels. See Figure 4 for levels and electrode numbering. In (a), the interelectrode distance (IED) increases when going to the right. In (b), the IED is 5 cm between *levels 1* and *2* and *levels 1* and *3*, and 10 cm between *levels 1* and *3*. The modeling data are in arbitrary units, so the unit of *y*-axis is mV [I].

5.2 The signal quality provided by new bipolar ECG leads

To evaluate whether the signal provided by small bipolar leads is strong enough for clinical utilization, we analyzed 120 bipolar leads in terms of QRS and P-wave amplitude in [II]. The amplitudes were calculated as an average from the BSPM ECG of 236 normal subjects. Figure 10 illustrates the average QRS and P-wave amplitudes for 120 bipolar leads (i.e., electrode pairs). The uppermost, middle, and bottom-most figures represent diagonal, vertical, and horizontal leads, respectively. Each graph includes leads from different rows on the chest denoted as, e.g., R 1-2 for diagonal and vertical leads and R 1 for horizontal leads. See Figure 5 (b) for row and electrode numbering.

The leads providing the highest amplitudes are indicated with filled squares. Generally, it was observed that the diagonal leads provided the best performance. This is logical, since these leads lie in the direction of the heart's main electrical activity. The highest QRS amplitudes (~2250 µV) were obtained from diagonal leads (electrode pairs) 37–45 and 44–52. The highest P-wave amplitudes (~100 µV) were obtained from diagonal leads 20–29 and 21–30.

If we assumed a reference noise level of 60 µV, the QRS amplitude was higher than the noise in all studied bipolar leads. However, with this noise level, the P-wave amplitude was too small in all horizontal and most diagonal and vertical leads. Only 8 leads between rows 2–3 and 6 leads between rows 3-4 provided P-wave amplitudes higher than 60 µV. However, when comparing the results with 15 µV, which represents a low noise situation, all studied leads provided a detectable P-wave and QRS-complex.

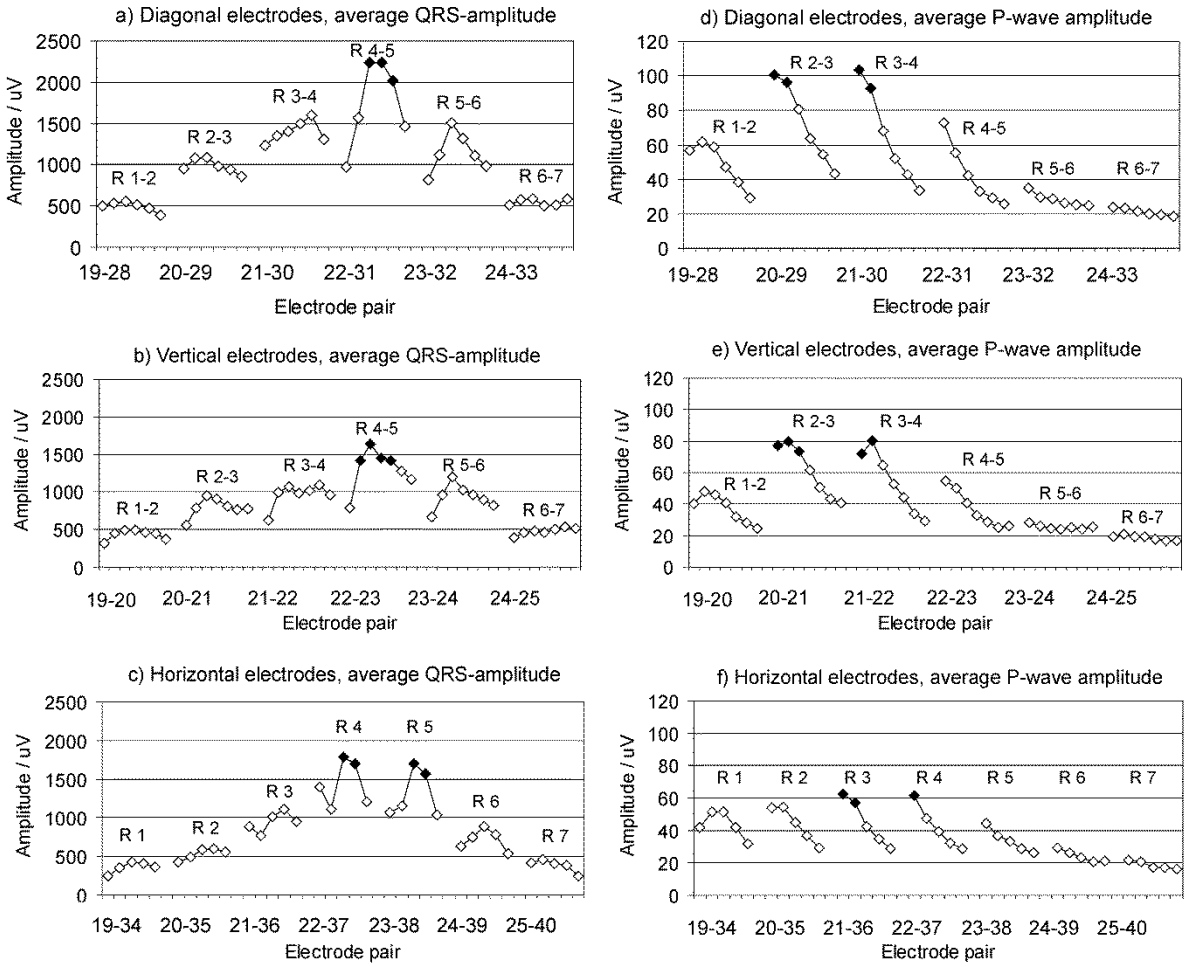

Figure 10. QRS (left column) and P-wave amplitudes (right column) obtained from 120 bipolar leads (electrode pairs) on the BSPM. The uppermost, middle, and bottom-most figures represent diagonal, vertical, and horizontal leads, respectively. The rows in which electrodes are located are indicated as R 1-2, R 2-3, etc. Each row includes six squares for diagonal, seven squares for vertical, and five squares for horizontal leads. On the *x*-axis, only the first lead is denoted for each row. When moving to the right on the graphical illustration, the lead is moving towards the left side of the subject's chest. The filled squares denote the leads providing the highest signal amplitudes. See Figure 4 for row and electrode numbering [II].

5.3 Optimal location for new bipolar ECG leads for healthy subjects

From the results in Figure 10, we can select the bipolar leads providing the highest QRS and P-wave amplitudes. These diagonal, vertical, and horizontal leads are further illustrated in Figure 11. The leads that maximize the QRS amplitude are depicted in black, and the leads that maximize the P-wave are depicted in gray.

It can be observed from Figure 11 that for all lead orientations, the leads located near standard precordial leads V2-V4 provided the highest QRS amplitudes. Correspondingly, the best area for P-wave detection was among or right above the chest electrodes of standard leads V1 and V2. Among the leads depicted in Figure 11, the highest QRS amplitudes were obtained from diagonal leads (electrode pairs) 37–45 and 44–52. Accordingly, the highest P-wave amplitudes were obtained from diagonal leads 20–29 and 21–30. See the electrode numbering in Figure 4 (b).

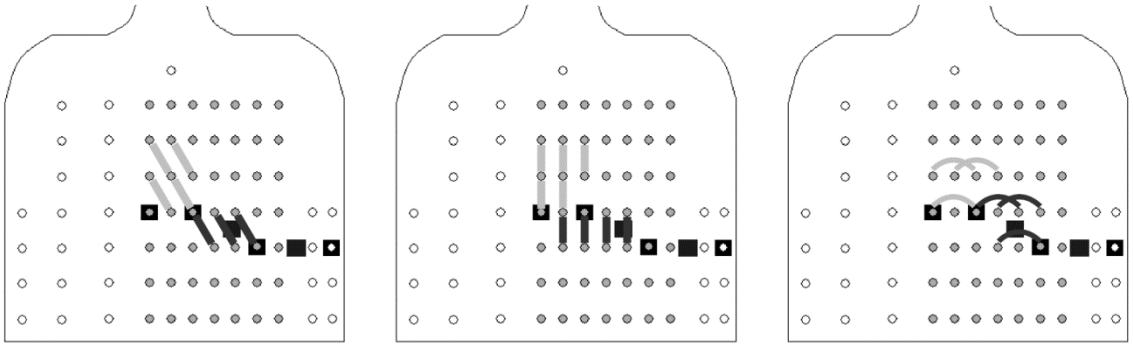

Figure 11. The (a) diagonal, (b) vertical, and (c) horizontal bipolar leads providing the highest QRS (black) and P-wave (grey) amplitudes. Black squares denote the location of the chest electrodes of standard 12-lead system leads V1-V6 [II].

5.4 The value of new bipolar ECG leads in diagnosing LVH and CAD

The previous chapters presented the performance of new bipolar leads by analyzing cases with normal ECG. This information is valuable when designing new monitoring devices for healthy subjects. This chapter introduces a more clinical point of view, specifically an analysis of the performance of new bipolar leads in detecting patients with LVH or CAD.

Detecting LVH patients

In [III], we evaluated whether closely separated (6 cm) bipolar leads can differentiate subjects with LVH from subjects with normal ECG. The material contained 120-lead BSPM ECGs from 236 normal and 116 LVH subjects. A total of 36 vertical, 30 horizontal, and 66 diagonal bipolar leads were studied (Figure 6). The average QRS amplitudes were calculated, and the leads' overall diagnostic performance was assessed by ROC analysis.

We found that the new bipolar leads are efficient in discriminating subjects with LVH from normal subjects. The leads providing good overall performance (ROC ≥ 0.70 or ROC ≤ 0.30) are illustrated in Figure 12. The classification rule for ROC areas 0.50 or greater was that LVH subjects have higher amplitudes, and the rule for ROC areas 0.50 or smaller was that healthy subjects have higher amplitudes. Multiple diagonal dL, diagonal dR, and vertical leads on the lower anterior thorax provided good (18, 24, and 30, ROC > 0.70) or very good (vertical 24, ROC > 0.80) overall performance. The performance of the lower horizontal leads (6, 24, and 30) was also good (ROC > 0.70). In addition, vertical leads 10 and 16, located higher on the thorax, provided a good overall diagnostic capacity, but with the opposite rule for the amplitude (ROC ≤ 0.30). This means that higher on the chest (e.g., lead 16), the average QRS amplitudes were lower in the LVH group than within normal subjects, whereas in the lower anterior area (e.g., lead 24), the opposite was the case. These QRS amplitude relationships are also illustrated in Figure 12 as light and dark grey areas.

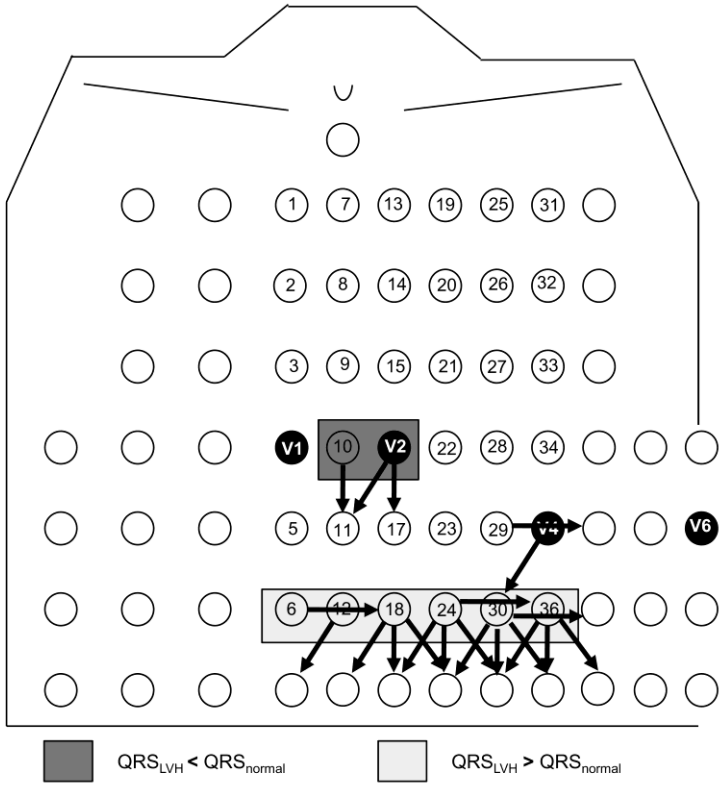

Figure 12. Best bipolar leads for detecting left ventricular hypertrophy (LVH). Arrows denote the location and orientation of each lead. These leads provided a good overall diagnostic performance in differentiating LVH subjects from normal subjects (ROC area ≥ 0.70). Modified from [III].

To compare the performance of the new bipolar leads with that of an existing LVH criterion, the ROC curves for the average QRS amplitude in two bipolar vertical leads (16 and 24) and for the traditional Sokolow-Lyon criterion are illustrated in Figure 13. In addition, the performance of QRS amplitude in bipolar lead locations 16 and 24 and of the Sokolow-Lyon criterion is further illustrated in Table 2, in which ROC areas, sensitivity values at 90% and 95% specificities, and cutoff values are listed. Locations 16 and 24 were selected, as they provided the highest overall performance of the studied bipolar leads. According to the ROC curves in Figure 13, the overall performances of bipolar vertical leads 16 and 24 are comparable to that of the Sokolow-Lyon criterion. Furthermore, it can be seen from Table 2 that the vertical and diagonal bipolar leads at location 24 provided similar or higher sensitivities in relation to the traditional Sokolow-Lyon criterion at both 90% and 95% specificities when differentiating LVH subjects from normal subjects. These leads had similar ROC areas (0.77–0.81) and cutoff points (1,030–1,060 µV), which means that with a bipolar lead located in this area, the direction is not that critical.

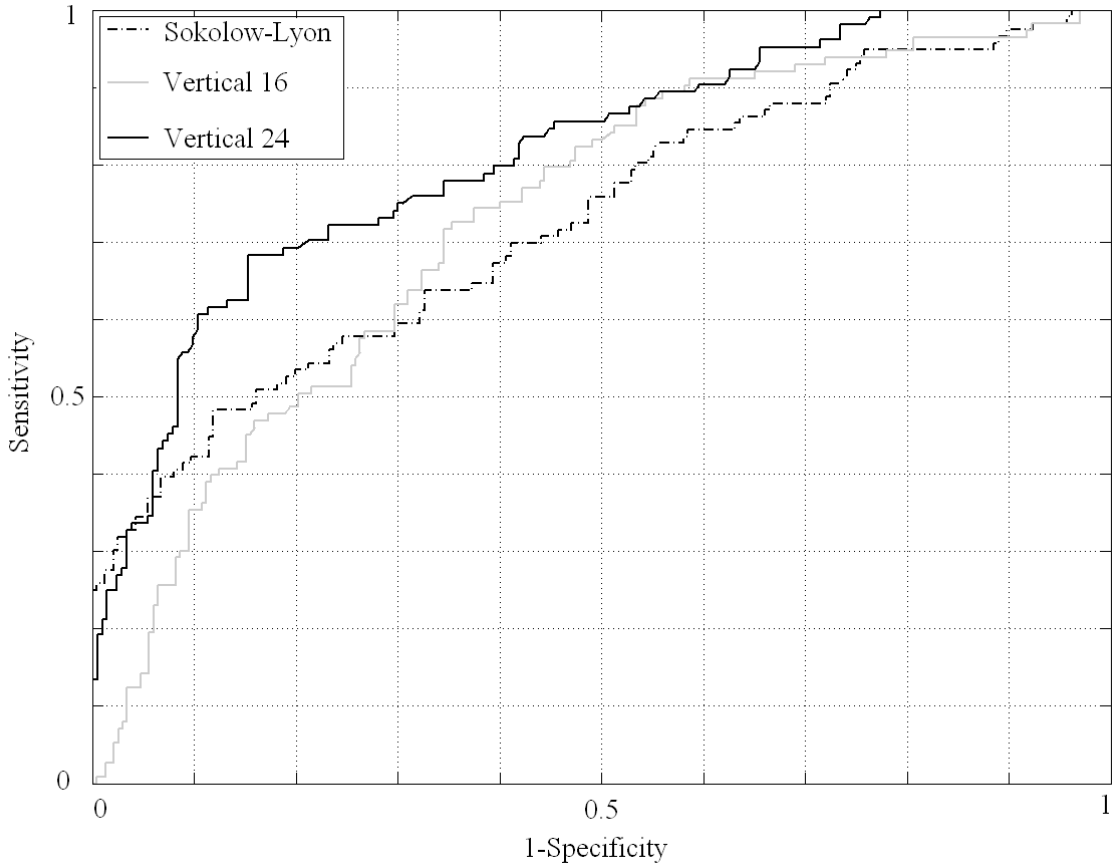

Figure 13. ROC curves to differentiate subjects with LVH from normal subjects. The QRS amplitude from bipolar vertical leads 16 and 24 and the Sokolow-Lyon criterion were used as variables [III].

Table 2. ROC area, sensitivity, and cutoff point at 90% and 95% specificities for QRS amplitude in bipolar lead locations 16 and 24 and for the Sokolow-Lyon criterion, comparing LVH subjects to normal subjects [III].

Lead	ROC area	Sensitivity at 90% specificity	Cutoff point (µV) at 90% specificity	Sensitivity at 95% specificity	Cutoff point (µV) at 95% specificity
Bipolar 16					
Vertical	0.27	35%	<816	14%	<558
Horizontal	0.54	22%	>2901	11%	>3250
Diagonal dL	0.32	27%	<1066	12%	<772
Diagonal dR	0.30	28%	<756	16%	<487
Bipolar 24					
Vertical	**0.81**	59%	>765	34%	>1054
Horizontal	0.72	42%	>1356	33%	>1654
Diagonal dL	**0.77**	49%	>860	37%	>1060
Diagonal dR	**0.79**	54%	>856	41%	>1030
Sokolow-Lyon (S_{V1}+$R_{V5/V6}$)	0.73	42%	>4255	35%	>4881

dL = diagonal downward left, dR = diagonal downward right. See Figure 6 for lead locations.

Detecting CAD patients

In [IV], our aim was to evaluate the diagnostic performance of leads CM5 and V4R in the detection of CAD. The material comprised 579 patients referred for a bicycle exercise ECG test in the Finnish Cardiovascular Study, and the patients were divided into three groups: angiographically proven CAD (CAD, n = 255), no CAD by angiography (NoCAD, n = 126), and low likelihood of CAD (LLC, n = 198). The diagnostic accuracy of leads CM5 and V4R was assessed with ROC analysis, and the parameter used in the analysis was maximum ST-depression at peak exercise. The ROC analysis was conducted for two group comparisons: CAD vs. LLC and CAD vs. NoCAD. The analysis was conducted both for individual leads and for lead sets, where V4R and CM5 were added to the standard lead system.

Individual leads

The ROC areas and the sensitivity and specificity values at -0.10 mV ST segment values for individual leads V5, CM5, and V4R are listed in Table 3, and the corresponding ROC curves are illustrated in Figure 14 (a). In Figure 14, the squares indicate -0.10 mV ST segment values, and the open and closed circles indicate -0.15 and -0.05 mV ST values, respectively. In both comparisons (CAD vs. LLC and CAD vs. NoCAD), the ROC areas obtained from lead CM5 (0.72 and 0.57) were comparable to those of lead V5 (0.72 and 0.58). At -0.10 mV ST-segment value, lead CM5 provided a higher sensitivity but lower specificity than lead V5. In addition, the ROC area, sensitivity, and specificity of lead CM5 were similar to those of the standard 12-lead system. The ROC areas obtained from lead V4R were smaller (0.61 and 0.53) than those of CM5 and V5, and the sensitivity of lead V4R was low (7%).

Among the individual leads, lead V5 gave the highest sensitivity (47%) at -0.10 mV ST-segment value.

Lead sets

The ROC areas and the sensitivity and specificity values at -0.10 mV ST segment values for the lead sets are listed in Table 3, and the corresponding ROC curves are illustrated in Figure 14 (b). It can be observed from this figure that adding lead CM5 to the standard leads did not change the ROC area but increased the sensitivity and decreased the specificity in both group comparisons. Adding lead V4R did not notably change the sensitivity or specificity, but decreased the ROC area.

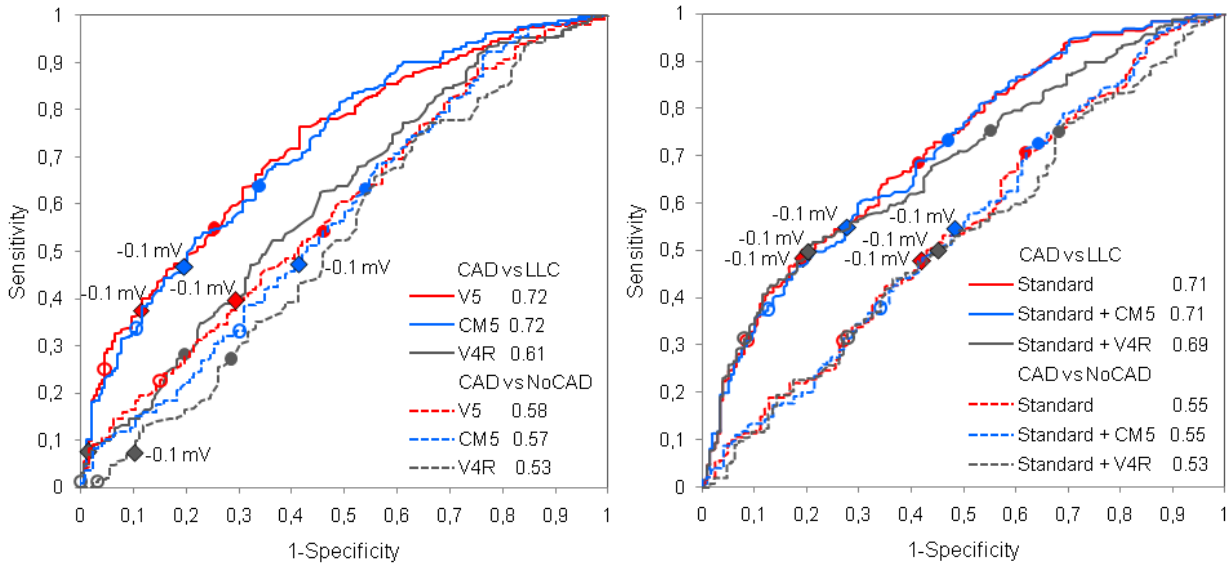

Figure 14. The ROC curves and areas under the curve for ST-depression at peak exercise recorded (a) from individual leads V5, CM5, and V4R, and (b) from the following lead sets: Standard, Standard + CM5, and Standard + V4R. Standard: Standard leads with the exclusion of V1 and aVL. Solid lines indicate comparison between coronary artery disease (CAD) and low likelihood of CAD (LLC) groups, and dashed lines indicate comparison between angiographically proven CAD and no-CAD (NoCAD) groups. The closed circles, squares, and open circles indicate ST-segment values of -0.05 mV, -0.10 mV, and -0.15 mV, respectively [IV].

Table 3. Diagnostic performance of individual leads V5, CM5, and V4R, and the lead sets. Modified from [IV].

	Individual leads			Lead sets		
	V5	CM5	V4R	Standard[a]	Standard + CM5	Standard + V4R
CAD vs. LLC						
ROC area	0.72	0.72	0.61	0.71	0.71	0.69
Sensitivity at -0.10 mV ST-segment value (%)	38	47	7	48	54	49
Specificity at -0.10 mV ST-segment value (%)	88	80	98	81	73	80
CAD vs. NoCAD						
ROC area	0.58	0.57	0.53	0.55	0.55	0.53
Sensitivity at -0.10 mV ST-segment value (%)	38	47	7	49	54	50
Specificity at -0.10 mV ST-segment value (%)	71	60	91	57	52	55

CAD = coronary artery disease, LLC = low likelihood of CAD

[a]Standard leads with the exclusion of V1 and aVL.

6. DISCUSSION

This chapter discusses the main results, findings, and limitations of our research. First, we address the results obtained from the modeling study. Second, we discuss whether short-distance bipolar leads can provide an ECG signal that is adequate for clinical utilization. Third, we recommend how those bipolar leads should be located in order to obtain the best ECG signal strength within healthy subjects. Fourth, we assess the value of new bipolar leads in diagnosing LVH and CAD. Finally, we discuss the value of new bipolar leads in future healthcare.

6.1 Modeling the sensitivity of new ECG leads

The purpose of this thesis was to study the properties of new bipolar ECG leads for wireless and wearable applications. One possible method for evaluating the performance of new electrode configurations is modeling the bioelectric fields with a computer model. However, it was unclear how well the modeled measuring sensitivity corresponds to the actual signal strength. To study the value of the modeling method, we compared the results from realistic 3D thorax models with clinical 120-lead BSPM data. Our results show that the measuring sensitivity modeled with realistic thorax models and with lead field method corresponds to the actual ECG signal strength. When modeling the unipolar leads, the correlation coefficient between Model 2 and BSPM data was $r = 0.86$ ($n = 117$, $p < 0.05$), which can be considered good correlation. In the case of bipolar electrode pairs, the correlation was lower, at $r = 0.62$ between Model 1 and BSPM data, and $r = 0.71$ between Model 2 and BSPM data. These results indicate that the unipolar leads are less sensitive to individual variation than the bipolar leads. This is probably because short bipolar leads are more localized and thus more sensitive to changes in the position, orientation, and electrical properties of the heart and other underlying tissues. In general, the modeling method was able to predict the relative changes in signal strength. However, in the left precordial area, the

clinical data gave higher values than modeling. This was due to the fact that the direction of the heart's electric axis, which normally slopes downwards left, increased the signal in the electrodes at the cardiac apex area. This increase was not seen in the models, as they are passive. This is one limitation of our models: They do not include the heart's electrical activity, but only take into account the tissue resistivities and geometries. Another limitation concerns the sensitivity distribution. Our calculations assume a uniform source over the heart muscle, but in the beating heart, the electric source is dynamic and constantly changing. On the other hand, a passive model has the benefit of providing more generalized results, as it is not confined to a certain condition. With increasing computing power, however, it may also be possible to include and more specifically define the cardiac activity into the models, thereby enhancing their accuracy in more specific cases.

One limitation of this study is that the models represented only the thorax anatomy of two individuals. Yet, the models were different from each other. Model 1 was made from cryosections, and represented a large person, whereas Model 2 was made from live MR images and represented a smaller person of Asian origin. From these two, Model 2 seemed to better predict the actual signal strength. This may have been related to the postmortem data of the VHM project or because the anatomy of the VHM model is far from being representative of the general population. However, along with developing image processing methods and computing power, it is possible to create individualized models based on MR or CT images. In this way, the properties of new recording leads could be tested individually for each person. Another future possibility is to create models representing a certain condition, such as LVH. Further modeling could include designing leads for a specific cardiac area, or monitoring the area of known arterial stenosis or the arrhythmogenic zone.

It should be noted that modeling does not give absolute signal strength values, but it does provide information on the relative changes in signal strength. Thus, modeling can be utilized when comparing different electrode locations. Another major benefit of modeling in general is that it provides a fast way of testing new electrode configurations. This is useful when designing wearable or wireless systems and choosing the appropriate electrode locations. We may conclude that the measuring sensitivity data computed from the realistic 3D thorax models will be useful when developing new electrode montages and measurement systems.

Regarding the BSPM data that were utilized in this thesis to validate the modeling results, the major limitation was that we did not have access to detailed patient characteristics such as age, gender, obesity, ethnicity, medication, and so on. However, as this study has a technical scope and focuses on evaluating the performance and comparing different ECG leads, we believe that the results are still useful, as the

number of subjects was high. Most importantly, the BSPM that we used offered an extensive ECG database for testing different electrode configurations and for evaluating the performance of new bipolar leads in both healthy and LVH subjects.

6.2 The signal quality provided by new bipolar ECG leads

Bipolar ECG leads have been utilized in a variety of wireless, wearable, and implantable ECG devices during the last decade. However, it is important to evaluate the signal quality provided by closely-spaced electrodes. The BSPM data on 236 normal subjects offers extensive data for testing different electrode configurations. By analyzing the average QRS and P-wave amplitudes on 120 bipolar leads on the anterior thorax, we found that most of the bipolar ECG leads with a short IED (approximately 6 cm) provided a detectable ECG signal in healthy subjects. The highest QRS (~2250 µV) and P-wave (~100 µV) amplitudes were obtained from diagonal leads located close to leads V2-V3 and leads V1-V2; respectively. It is logical that the diagonal leads record the strongest signal, as the main cardiac activity is usually directed diagonally, and the strongest signal is projected to the lead parallel to the activation front. In contrast, the lowest signal strength was obtained from horizontal bipolar leads. Further, all leads located on the highest or lowest rows on the chest provided a poor signal strength.

The results were also compared to reference noise levels of 15 µV and 60 µV. The QRS amplitude was higher than 60 µV in all bipolar leads, which means that for applications requiring only the detection of HR, all studied bipolar leads are adequate. The P-wave amplitudes were higher than 60 µV in only 14 of the studied leads. These leads were located above the precordial electrodes of standard leads V1-V2. Nevertheless, in comparison with a reference noise level of 15 µV, all studied bipolar leads provided a detectable P-wave. A recent thesis (Väisänen 2008) reported that the measurement noise can be reduced to a level of 1–4 μV_{rms}. These measurements were conducted in a normal unshielded laboratory, and thus these levels should be achievable in most measurement environments. Nevertheless, the noise created by movement and muscle activity is usually higher, especially when measuring a mobile person. Thus, the required signal level depends on the application, the measurement environment, and the movement artifacts.

6.3 Optimal location for new bipolar ECG leads for healthy subjects

As mentioned in the previous chapter, the bipolar leads directed diagonally provided the highest QRS and P-wave amplitudes. In contrast, the lowest amplitudes were obtained from horizontal leads. The results also showed that the best location for QRS

complex is around the chest electrodes of the standard precordial leads V2, V3, and V4, and that the optimal location for P-wave detection is above the chest electrodes of leads V1 and V2. This result is logical, since QRS complex arises from ventricular and P-wave from atrial activation. Similarly, based on their measurements, Fensli et al. (Fensli 2004) reported that the optimal position for their plaster-like ECG sensor (IED 3 cm) is in the 4^{th} and 5^{th} intercostal spaces at the apex of the heart. Our results regarding the detection of QRS complex support this finding, as the chest electrodes of leads V3 and V4 lie in the same area.

It should be noted that in our study, the amplitudes were calculated as an average from 236 subjects, and the recorded signal strength varied among different individuals. However, the findings give an indication of the optimal location for a small ECG device for different purposes. If the aim is to detect the HR or to concentrate on the QRS complex, then the optimal location is likely to be that providing the highest QRS amplitude. In the case of classifying cardiac arrhythmias, such as atrial fibrillation (AF), the location providing highest P-wave amplitude is probably the best choice. This information will be useful when designing the electrode locations for a small wireless, wearable, or implantable ECG device.

Another interesting aspect regarding wearable systems would be identifying the best combination of 2 to 3 bipolar leads or using classification methods other than pure amplitude. Recently, Tomašić et al. introduced a multivariate linear regression based synthesis of 12-lead ECG from three bipolar leads (Tomašić 2010). They reported that their study was motivated by our results of publication [I], which showed that a bipolar lead with 6 cm interelectrode distance provides an acceptable S/N ratio. In a further publication by Trobec et al., the researchers analyzed sets of two, three, and four differential leads, and concluded that just three bipolar leads suffice for reliable synthesis of the 12-lead ECG (Trobec 2011). The best locations for healthy subjects corresponded to three bipolar leads—(41, 43), (43, 59), and (59, 61) in Figure 4(b). Their results support the assumption that closely spaced bipolar leads provide an adequate representation of the heart's electrical activity, and that new precordial bipolar leads have potential in future healthcare.

6.4 The value of new bipolar ECG leads in diagnosing LVH and CAD

So far, we have found that a correctly positioned small bipolar ECG lead is able to provide sufficient signal amplitude to detect the main parameters of ECG. After this, we wanted to test the value of small bipolar leads in diagnosing cardiovascular conditions. LVH and CAD were chosen because they are among the main

cardiovascular diseases and our data provided information on patients with these conditions. The results are discussed below.

Left ventricular hypertrophy (LVH)
When analyzing the BSPM of 236 normal and 116 LVH subjects, it was observed that new closely spaced bipolar leads are able to detect subjects with LVH. Furthermore, the performance of the best bipolar leads was similar to that of the traditional Sokolow-Lyon criterion. Another major finding was that the bipolar leads with the best overall diagnostic performance were located in two areas, one near the precordial electrodes of standard leads V1 to V3, and the other on lower anterior thorax (Figure 12). It was interesting to see that the classification rule was different in these two areas. In the bipolar leads located lower on the thorax, the QRS amplitudes were higher in the LVH group than within normal subjects. In contrast, in the bipolar leads located near the precordial electrodes of V1-V3, the QRS amplitude was lower in the LVH group than within normal subjects. Generally, the opposite is the case, as LVH is associated with high QRS voltages in the precordial unipolar leads V1, V2, V5, and V6.

The reason for the lower amplitudes in the new precordial bipolar leads could be that the thickening of the left ventricular wall enhances all body surface potentials in the precordial area, thereby decreasing the potential difference detected by two closely lying bipolar lead electrodes. Another possible reason is that the shifting of the QRS axis related to LVH shortens the projection detected by the bipolar leads, hence inducing smaller amplitudes. It is known that LVH causes the QRS frontal axis to shift slightly leftward and the QRS transversal axis to shift markedly posteriorly (Wagner 2007). Furthermore, a recent modeling study suggested that it is a combination of anatomical and electric remodeling that creates the QRS complex changes seen in LVH patients (Bacharova 2009).

Regarding the complex changes involved in LVH, we conducted a further study on short bipolar leads by including a so-called complex LVH group in the analysis (Väisänen 2010). The study population consisted of 236 healthy subjects, 116 pure LVH patients with either pure left-sided valvular disease or sustained hypertension (150/90 mmHg or higher) and 189 complex LVH patients with various cardiac conditions frequently associated with LVH (Kornreich 1993). We found that the best bipolar leads provided a better overall performance (normal vs. complex, ROC=0.85; normal vs. pure, ROC=0.81) than the traditional Sokolow-Lyon method (normal vs. complex, ROC=0.67; normal vs. pure, ROC=0.73). The QRS amplitude criteria were different, and the ROC areas were higher when differentiating complex LVH patients from normal patients than when differentiating pure LVH patients from normal patients. These results support our previous finding that precordial bipolar leads with a

short IED can discriminate subjects with LVH from normal subjects. Our results also indicate that the ECG changes in LVH vary depending on the type of LVH (pure vs. complex), which makes the diagnosis more challenging. There are certain limitations to our study on LVH. In the dataset, the male and female patients were not separated, so we cannot state how gender affects the performance of bipolar leads. It should also be noted that although large voltage differences were noticed between normal subjects and subjects with LVH, there is also large interindividual variability.

In general, the results of this thesis show that new small precordial bipolar leads could provide advanced tools for LVH diagnostic. These new leads cannot replace the standard 12-lead system, but they can give additional value, especially in wearable or implantable long-term measurements. In the future, it would be interesting to analyze the performance of bipolar leads further by identifying the best combination of 2 or 3 bipolar leads. Utilizing multiple leads would have the advantage of allowing changes to be sensed in different directions. Another interesting area would be to apply other classification methods than pure amplitude, such as time-voltage QRS area.

Regarding the use of short bipolar leads in other cardiac conditions, Arzbaecher et al. (Arzbaecher 2006) reported that ECGs recorded by a small subcutaneous monitor (interelectrode distance 4 cm) are of sufficient quality and amplitude to allow accurate detection of VT/VF. Further, the performance of closely spaced bipolar leads in ischemia detection has been reported by Song et al. (Song 2004). These studies support our finding on the applicability of small, closely spaced bipolar leads in ECG analysis.

Coronary artery disease (CAD)

Among CAD patients, the maximal ST depression most commonly occurred in leads V5 and V6, regardless of disease location and severity (Mason 1967; Fuchs 1982). It has been reported by Viik et al. (Viik 1997; Viik 1998) that in addition to leads V5 and V6, leads I and -aVR also exhibit high performance when differentiating between patients with CAD and patients with a low likelihood of the disease. This indicates that the importance of leads I and -aVR has been undervalued. The benefit of leads V5 and V6 is that the signal amplitude is high in that area. In leads -aVR and I, the amplitude is lower, so that the effective use of these leads requires a 50% smaller partition value than that used in the lateral precordial leads (e.g., -0.05 mV ST depression). It is worth noting that leads –aVR and CM5 have a quite similar lead vector direction in the frontal plane. Regarding lead CM5, based on 100 male subjects, Chaitman et al. (Chaitman 1978) have reported that incorporating leads CM5, CC5, and CL with standard leads improves the sensitivity and efficiency of the maximal treadmill exercise test. Correspondingly, our study with both male and female subjects showed that when adding lead CM5 with standard leads, the specificity decreases, but the ROC

area remains the same and the sensitivity increases. These results indicate that bipolar lead CM5 could be useful in applications where high sensitivity is emphasized. Regarding lead V4R, Michaelides et al. have stated that the use of right precordial unipolar leads along with the standard six precordial leads greatly improves the sensitivity of exercise testing for the diagnosis of CAD (Michaelides 1999). However, our results do not support this finding, as in our study, adding lead V4R to the standard lead system did not notably change the sensitivity or specificity, but decreased the ROC area.

Bowles et al. (Bowles 1985) compared the results obtained from 18 unipolar precordial leads and those from bipolar leads CM5 and CC5. The data included 21 patients with severe angina and luminal narrowing of at least 70% in one or more major coronary arteries. In all cases the ST depression exceeded 1 mm in both CM5 and CC5 at the peak of exercise. The magnitude of ST depression was greater in the bipolar leads in 75% of cases and in the remaining 25% the greatest peak ST depression occurred in a single unipolar lead. Again, Guiteras et al. (Guiteras 1982) studied the diagnostic accuracy of 14-lead exercise electrocardiography in 112 women who had no history of myocardial infarction and underwent coronary angiography. The sensitivity of ST-segment displacement of 0.1 mV or more in any of studied ECG leads was 79% for coronary artery stenosis of at least 70%, and the specificity was 66%. Results were similar using bipolar ECG leads CC5 and CM5 or 11 standard ECG leads (excluding aVR). In our results, including both males and females, we also found that the performance of lead CM5 is similar to both that of standard lead V5 and that of 10 standard leads (excluding V1 and aVR). When analyzing single leads, CM5 gave a lower specificity but a higher sensitivity and a similar ROC area than lead V5. This means that CM5 detects more CAD patients than V5. Furthermore, the sensitivity, specificity, and ROC area of CM5 were similar to that of 10 standard leads. Based on this, it could even be concluded that a single lead CM5 is enough for CAD detection. In the future, lead CM5 may be especially valuable in wireless or wearable applications, as the lead's location enables it to be integrated into a t-shirt and the measurement field encompasses the precordial area. One commercial solution benefiting from wearable ECG measurement is the Finnish CorusCardio concept by CorusFit Oy (CorusFit ; Vehkaoja 2008). This company's preventive and rehabilitation programs and methods can be applied among people at risk for or already diagnosed with CAD. One of the bipolar leads integrated into the CorusFit WiEKG and SensorWear is similar to lead CM5. Our results further support the use of this lead in wearable or wireless cardiac solutions.

6.5 The value of new bipolar leads in future healthcare

This thesis assessed the value of new bipolar leads in different applications, specifically general ECG recording within healthy subjects and detecting ECG changes in the cardiovascular diseases LVH and CAD. The specific conclusions of this thesis are introduced in the following chapter. To sum up, our main findings were that a closely spaced (5–6 cm) bipolar lead provides a strong ECG signal within healthy subjects, and is also able to detect LVH patients when the lead is correctly positioned on the thorax. We also found that the performance of bipolar lead CM5 is similar to that of standard lead V5 and that of 10 standard leads (excluding V1 and aVR) in detecting CAD patients with exercise ECG. These results show that the new bipolar leads work surprisingly well, both when monitoring the normal ECG and when detecting cardiac conditions.

These new bipolar leads can be utilized in the wireless, portable, or implantable devices that have been emerging during the past decade. Wireless solutions in healthcare can improve the patient care, reduce costs, and enable individuals to take more active approach to their health. Wireless remote monitoring could, for example, add value to athletes' training, increase the safety of elderly people living at home, and enable monitoring of patients suffering from paroxysmal atrial fibrillation or angina pectoris. With small, unobtrusive ECG devices, it would be possible to detect events that are currently missed, as the episode might be over when the individual arrives at the healthcare center. In the future, it might even be possible for patients to interface with their doctors through, e.g., a smartphone.

The additional value of small bipolar leads is that they enable the development of lightweight measurement devices. Along with the improvements in electronics design, it is possible to generate devices—including electrodes, measurement electronics, and wireless signal transfer—in a small, plaster-like device. The small size and absence of lead wires improve patient comfort and reduce motion artifacts. Further, the possibility of integrating monitoring devices into clothing enables new ways of monitoring cardiac activity. These novel, wearable devices permit the acquisition of ECG signals for a variety of applications ranging from emergency care to long-term monitoring at home. Further, with increasing computing power, more sophisticated patient monitoring ECG devices can be developed. One important application where bipolar electrodes are already utilized is implantable monitoring, such as the cardiac event monitors by Medtronic (Medtronic) and St. Jude Medical (StJudeMedical).

Another benefit of the bipolar leads is the modifiable measurement field. The standard 12-lead system precordial leads are referred to WCT and detect electrical changes in a large volume. The measurement field of closely spaced bipolar leads lies within a smaller volume, and thus can be targeted to detect changes in a certain area. This could

allow us to develop leads tailored to a certain condition, for a certain individual, or to detect changes in atrium or ventricle. In other words, as the 12-lead system is a widely utilized standard measurement of cardiac function, small bipolar leads can be designed to give more specific information. Further, short bipolar leads can also be derived from the standard 12-lead system electrodes. Including these short bipolar leads in the analysis could give additional value to the diagnostics.

One limitation of small, portable ECG systems is the limited number of leads. Moreover, the short lead vectors and close proximity to the heart result in ECG amplitudes and morphologies that differ from more familiar recording techniques. These changes in the measured ECG affect the outcome of the diagnosis. Thus, the application of new bipolar ECG leads requires new criteria to be set for diagnostics. Hence, further research on the signals and parameters provided by novel bipolar leads is needed in order to apply them in clinical use.

What kind of research is needed for these systems to become widespread? First, the devices need to be user-friendly, lightweight, portable, and provide data in real time, before they will gain public acceptance. In particular, the user interfaces should be convenient and easy to use. It would also be beneficial if the new wearable systems could be integrated with the existing measurement platforms. To distinguish between different users, the signals should be identified, and a high level of security is needed when dealing with healthcare data. Further, real-time signal analysis would be beneficial in order to, e.g., detect cardiac events. In addition, the healthcare systems and databases need to be developed so that the service behind these devices is also available, e.g., a doctor interpreting the signals and acting accordingly.

Regarding wearable textiles and mobile measurement in general, one of the main challenges involves reducing movement artifacts and ensuring stable contact between the skin and the recording electrode. One of the limitations of this thesis is that most of our ECG data were collected in a static position. The mobile aspect was involved only in the exercise ECG data. However, the purpose of this thesis was to concentrate on the hardware aspect and electrode placing. A natural extension of this work would be to collect mobile ECG data in different circumstances, and to develop adaptive signal processing algorithms that compensate for the physical movements of the subject. Finally, although this thesis gives new information on the performance of small bipolar ECG leads, further research among different populations and in different circumstances is required before such ECG systems become widely accepted among clinicians.

The 12-lead ECG still remains the main diagnostic tool for heart disease, as no other technique has gained such widespread and sustained acceptance. Yet, new lead

systems are being developed and investigated. Novel, closely spaced bipolar leads can give new information to electrocardiology because they detect different types of changes in the ECG signal than standard leads. The challenge is that the standard 12-lead system is so widely accepted that the new possible lead configurations are still far from everyday use. However, the results of this thesis are promising and indicate that in the future, novel wearable or implantable monitors can be offered as new tools for ECG diagnostics.

7. CONCLUSIONS

According to the specific aims of the study, the following conclusions were made:

1. The results of lead field modeling analysis [I] demonstrated that the modeled measuring sensitivities correlated with the actual measured ECG data. Modeling provided information on the relative changes in the ECG signal strength when changing the electrode location and IED. Thus, lead field–based analysis of realistic, 3D thorax models provides an additional tool for the design of new ECG leads, e.g., for wireless or implantable solutions.

2. All studied bipolar ECG leads with a short IED (approximately 6 cm) provided a detectable signal when compared to a low noise level of 15 µV and considering the P-wave as the smallest parameter [II]. With a higher noise level of 60 µV, only certain bipolar leads oriented diagonally or vertically provided detection of the P-wave. However, the QRS complex was detectable in all studied leads.

3. The optimal orientation for a bipolar lead with a short IED was diagonally on the chest [II]. The best locations regarding the QRS complex and P-waves were around the chest electrodes of the standard precordial leads V2, V3, and V4, and above the chest electrodes of leads V1 and V2, respectively.

4. In clinical evaluation, it was found bipolar ECG leads with a short IED were able to discriminate between subjects with LVH and healthy subjects [III]. Moreover, vertical and diagonal bipolar leads on the lower anterior thorax provided similar overall diagnostic performance to the traditional Sokolow-Lyon method. Considering the additional bipolar lead CM5 in CAD diagnostics, we found that the performance of this lead is comparable to that of standard lead V5 [IV]. Further, by

adding lead CM5 to the standard 12-lead system, the sensitivity of the exercise test was increased.

This study consisted of modeling the sensitivity, optimizing the location, and evaluating the clinical performance of new bipolar ECG leads. We may conclude that modeling can be useful, especially in cases where in vivo measurements are impossible, such as in the design of implantable applications. Based on actual ECG data, it was observed that when correctly positioned, the short IED bipolar leads provide an ECG where all the parameters are detectable. Moreover, in selected clinical applications—LVH and CAD—the performance of the new bipolar leads was surprisingly good, as it was comparable or even better than those of the methods commonly used today. These results indicate that when correctly positioned, short IED bipolar leads are useful and can even give additional value for clinical diagnostics. In general, this thesis gives new information on the performance and value of small bipolar ECG leads, and consequently facilitates and contributes to the development of new wireless and portable measurement devices for general use as well as for clinical diagnostics.

8. REFERENCES

Ackerman, M. J. (1991). The Visible Human Project. *J Biocommun* 18(2): 14.

AliveCor Inc. Retrieved 20.05.2012, from http://alivecor.com/.

Altman, D. G. and J. M. Bland (1994). Statistics Notes: Diagnostic tests 1: sensitivity and specificity. *BMJ* 308(6943): 1552.

Anliker, U., J. A. Ward, P. Lukowicz, G. Tröster, F. Dolveck, M. Baer, F. Keita, E. Schenker, F. Catarsi, L. Coluccini, A. Belardinelli, D. Shklarski, M. Alon, E. Hirt, R. Schmid and M. Vuskovic (2004). AMON: A Wearable Multiparameter Medical Monitoring and Alert System. *IEEE Trans Inf Tech Biomed* 8(4): 415-27.

Arzbaecher, R., J. Jenkins, M. Burke, Z. Song and M. Garrett (2006). Database testing of a subcutaneous monitor with wireless alarm. *J Electrocardiol* 39 Suppl(4): S50-3.

Bacharova, L., V. Szathmary, M. Kovalcik and A. Mateasik (2009). Effect of changes in left ventricular anatomy and conduction velocity on the QRS voltage and morphology in left ventricular hypertrophy: a model study. *J Electrocardiol* 43(3): 200-8.

Benditt, D. G., C. Ermis, S. Pham, L. Hiltner, A. Vrudney, K. G. Lurie and S. Sakaguchi (2003). Implantable diagnostic monitoring devices for evaluation of syncope, and tachy and brady-arrhytmias. *J Interv Card Electrophysiol* 9(2): 137-44.

BlackBerry. Retrieved 20.04.2012, from http://worldwide.blackberry.com/.

Bowles, M. J., N. S. Khurmi, A. B. Davies and E. B. Raftery (1985). Multiple unipolar lead electrocardiographic monitoring during exercise in severe coronary artery disease: a comparison with bipolar lead monitoring. *Int J Cardiol* 9(2): 199-209.

Braat, S. H., J. H. Kingma, P. Brugada and H. J. Wellens (1985). Value of lead V4R in exercise testing to predict proximal stenosis of the right coronary artery. *J Am Coll Cardiol* 5: 1308-11.

Burke, M. C., Z. Song, J. Jenkins, M. Alberts, J. Del Priore and R. Arzbaecher (2003). Analysis of electrocardiograms for subcutaneous monitors. *J Electrocardiol* 36 Suppl: 227-32.

CardioNet Inc. Retrieved 30.05.2012, from http://www.cardionet.com/.

Casale, P. N., R. B. Devereux, P. Kligfield, R. R. Eisenberg, D. H. Miller, B. S. Chadhary and M. C. Phillips (1985). Electrocardiographic detection of left ventricular hypertrophy: Development and prospective validation of improved criteria. *J Am Coll Cardiol* 6: 572-80.

Casale, P. N., R. B. Devereux, M. Milner, G. Zullo, G. A. Harshfield, T. G. Pickering and J. H. Laragh (1986). Value of echocardiographic measurement of left ventricular mass in predicting cardiovascular morbid events in hypertensive men. *Ann Intern Med* 105: 173-8.

Chaitman, B. R., M. G. Bourassa, P. Wagniart, F. Corbara and R. J. Ferguson (1978). Improved efficiency of treadmill exercise testing using a multiple lead ECG system and basic hemodynamic exercise response. *Circulation* 57(1): 71-9.

Chi, Y. M., T.-P. Jung and G. Cauwenberghs (2010). Dry-contact and noncontact biopotential electrodes: methodological review. *IEEE Rev Biomed Eng* 3: 106-19.

Chiu, R.-D. and S.-H. Wu (2011). A BAN system for realtime ECG monitoring: from wired to wireless measurements. *IEEE Wireless Communications and Networking Conference (WCNC)*, Cancun, Mexico.

Chouhan, L., R. J. Krone, A. Keller and G. E. G (1989). Utility of lead V4R in exercise testing for detection of coronary artery disease. *Am J Cardiol* 64: 938-9.

CorusFit Oy. Retrieved 06.06.2012, from http://www.corusfit.fi/.

Crawford, M. H., S. J. Bernstein, P. C. Deedwania, J. P. DiMarco, K. J. Ferrick, A. J. Garson, L. A. G. LA, H. L. Greene, M. J. S. MJ, P. H. Stone, C. M. Tracy, R. J. Gibbons, J. S. Alpert, K. A. Eagle, T. J. Gardner, G. Gregoratos, R. O. Russell, T. J. Ryan and S. C. J. Smith (1999). ACC/AHA guidelines for ambulatory electrocardiography: executive summary and recommendations. A report of the American College of Cardiology/American Heart Association Task Force on Practice Guidelines (Committee to Revise the Guidelines for Ambulatory Electrocardiography). *Circulation* 100(8): 886-93.

Cömert, A., M. Honkala, M. Puurtinen and M. Perhonen (2008). The suitability of silver yarn electrodes for mobile EKG monitoring. *14th Nordic-Baltic Conference on Biomedical Engineering and Medical Physics*, Riga, Latvia.

DAVITA Medizinische Produkte GmbH & Co. Retrieved 20.01.2012, from http://www.davita-shop.co.uk/ecg-instruments.html.

DeVaul, R., M. Sung, J. GIbs and A. Pentland (2003). MIThril 2003: Applications and architecture. *Seventh IEEE International Symposium on Wearable Computers (ISWC'03)*, White Plains, New York, USA.

Draper, N. R. and H. Smith (1998). Applied regression analysis. New York, John Wiley & Sons, Inc.

Dunn, O. J. and V. A. Clark (1974). Applied statistics: Analysis of variance and regression. New York, John Wiley & Sons Inc.

Farwell, D. J., N. Freemantle and A. N. Sulke (2004). Use of implantable loop recorders in the diagnosis and management of syncope. *Eur Heart J* 25(14): 1257-63.

Fensli, R., E. Gunnarson and O. Hejlesen (2004). A wireless ECG system for continuous event recording and communication to a clinical alarm station. *26th Annual International Conference of the IEEE Engineering in Medicine and Biology Society (EMBS '04)*, San Francisco, USA.

Fernandez, M. and R. Pallas-Areny (2000). Ag-AgCl electrode noise in high-resolution ECG measurements. *Biomed Instrum Technol* 34(2): 125-30.

Finlay, D. D., C. D. Nugent, M. P. Donnelly, P. J. McCullagh and N. D. Black (2008). Optimal electrocardiographic lead systems: practical scenarios in smart clothing and wearable health systems. *IEEE Trans Inf Tech Biomed* 12(4): 433-41.

Fletcher, G. F., G. Balady, V. F. Froelicher, L. H. Hartley, W. L. Haskell and M. L. Pollock (1995). Exercise Standards : A Statement for Healthcare Professionals From the American Heart Association. *Circulation* 91(2): 580-615.

Flores-Mangas, F. and N. Oliver (2005) "Healthgear: A real-time wearable system for monitoring and analyzing physiological signals." Tech. rep. MSR-TR-2005-182, Microsoft Research.

Fox, R., A.-H. Hakki, A. Iskandrian and J. Hackney (1984). Relation between electrocardiographic and scintigraphic location of myocardial ischemia during exercise in one-vessel coronary artery disease. *Am J Cardiol* 53: 1529-31.

Frank, E. (1954). The image surface of a homogeneous torso. *Am Heart J* 47: 757-68.

Frank, E. (1956). An accurate, clinically practical system for spatial vectorcardiography. *Circulation* 13(5): 737-49.

Froelicher, V. F. and J. N. Myers (2000). Exercise and the Heart. Philadelphia, Pennsylvania, W.B. Saunders Company.

Fuchs, R. M., S. C. Achuff, L. Grunwald, F. C. Yin and L. S. Griffith (1982). Electrocardiographic localization of coronary artery narrowings: studied during myocardial ischemia and infarction in patients with one-vessel disease. *Circulation* 66: 1168-76.

Fulford-Jones, T. R. F., W. Gu-Yeon and M. Welsh (2004). A portable, low-power, wireless two-lead EKG system. *26th Annual International Conference of the IEEE Engineering in Medicine and Biology Society (EMBS '04)*, San Francisco, USA.

Gale, T. J., P. R. Johnston, D. Kilpatrick and P. M. Nickolls (1994). Implantable defibrillator electrode comparison using a boundary element model. *Proceedings of the 16th Annual International Conference of the IEEE Engineering Advances: New Opportunities for Biomedical Engineers*, Baltimore, MD USA.

Gianrossi, R., R. Detrano, D. Mulvihill, K. Lehmann, P. Dubach, A. Colombo, D. McArthur and V. Froelicher (1989). Exercise-induced ST depression in the diagnosis of coronary artery disease: a meta-analysis. *Circulation* 80: 87-98.

Grossmann, P. (2004). The LifeShirt: A multi-function ambulatory system monitoring health, disease, and medical intervention in the real world. In A. Lymberis and D. deRossi, Eds. Wearable ehealth systems for personalised health management: state of the art and future challenges. Amsterdam, IOS Press**:** 133-41.

Guiteras, P., B. R. Chaitman, D. D. Waters, M. G. Bourassa, H. M. Scholl, R. J. Ferguson and P. Wagniart (1982). Diagnostic accuracy of exercise ECG lead systems in clinical subsets of women. *Circulation* 65(7): 1465-74.

Gyselinckx, B., J. Penders and R. Vullers (2007). Potential and challenges of body area networks for cardiac monitoring. *J Electrocardiol* 40(6 Suppl): S165-8.

Hancock, E. W., B. J. Deal, D. M. Mirvis, P. Okin, P. Kligfield and L. S. Gettes (2009). AHA/ACCF/HRS Recommendations for the Standardization and Interpretation of the Electrocardiogram. Part V: Electrocardiogram Changes Associated With Cardiac Chamber Hypertrophy. *Circulation* 119: e251-61.

Hanley, J. A. and B. J. McNeil (1982). The meaning and use of the area under a receiver operating characteristic (ROC) curve. *Radiology* 143: 29-36.

Hoekema, R. (1999). The Interindividual Variability of the Electrocardiogram, Katholieke Universiteit Nijmengen. Doctoral Dissertation.

Huigen, E., A. Peper and C. A. Grimbergen (2002). Investigation into the origin of the noise of surface electrodes. *Med Biol Eng Comput* 40(3): 332-8.

Hyttinen, J. (1994). Development of Regional Aimed ECG Leads Especially for Myocardial Ischemia Diagnosis, Tampere University of Technology. Doctoral Dissertation.

Hyttinen, J., H. Puurtinen, P. Kauppinen, J. Nousiainen, P. Laarne and J. Malmivuo (2000). On the effects of model errors on forward and inverse ECG problems. *International Journal of Bioelectromagnetism* 2(2).

Jafari, R., A. Encarnacao, A. Zahoory, F. Dabiri, H. Noshadi and M. Sarrafzadeh (2005). Wireless sensor networks for health monitoring. *2nd ACM/IEEE International Conference on Mobile and Ubiquitous Systems*, San Diego, CA, USA.

Jain, A. and D. R. Murray (1995). Detection of myocardial ischemia. *Curr Probl Cardiol* 20: 773-824.

Kauppinen, P. (2000). Application of lead field theory in the analysis and development of impedance cardiography, Tampere University of Technology. Doctoral Dissertation.

Kauppinen, P., J. Hyttinen, T. Heinonen and J. Malmivuo (1998). Detailed model of the thorax as a volume conductor based on the visible human man data. *J Med Eng Technol* 22(3): 126-33.

Kauppinen, P., J. Hyttinen, P. Laarne and J. Malmivuo (1999). A software implementation for detailed volume conductor modelling in electrophysiology using finite difference method. *Comput Methods Programs Biomed* 58: 191-203.

Kauppinen, P., T. Kööbi, S. Kaukinen, J. Hyttinen and J. Malmivuo (1999). Application of computer modelling and lead field theory in developing multiple aimed impedance cardiography measurements. *J Med Eng Technol* 23(5): 169-77.

Koren, M. J., R. B. Devereux, P. N. Casale, D. D. Savage and J. H. Laragh (1991). Relation of left ventricular mass and geometry to morbidity and mortality in uncomplicated essential hypertension. *Ann Intern Med* 114: 345-52.

Kornreich, F. (1997). Clinical utility of body surface potential mapping. *Card Electrophysiol Rev* 3: 304-7.

Kornreich, F. (1998). Identification of best electrocardiographic leads for diagnosing acute myocardial ischemia. *J Electrocardiol* 31 Suppl: 157-63.

Kornreich, F., R. S. MacLeod and R. L. Lux (2008). Supplemented standard 12-lead electrocardiogram for optimal diagnosis and reconstruction of significant body surface map patterns. *J Electrocardiol* 41(3): 251-6.

Kornreich, F., T. J. Montague, M. Kavadis, P. Rautaharju, M. B. Horácek and B. Taccardi (1989). Multigroup diagnosis of body surface potential maps. *J Electrocardiol* 22 Supplement: 169-78.

Kornreich, F., T. J. Montague and P. M. Rautaharju (1991). Identification of first acute Q wave and non-Q wave myocardial infarction by multivariate analysis of body surface potential maps. *Circulation* 84: 2442-53.

Kornreich, F., T. J. Montague and P. M. Rautaharju (1993). Body surface potential mapping of ST segment changes in acute myocardial infarction. *Circulation* 87: 773-82.

Kornreich, F., T. J. Montague, P. M. Rautaharju, M. Kavadias and M. B. Horacek (1988). Identification of best electrocardiographic leads for diagnosing left ventricular hypertrophy by statistical analysis of body surface potential maps. *Am J Cardiol* 62(17): 1285-91.

Kornreich, F., T. J. Montague, P. M. Rautaharju, M. Kavadias, M. B. Horacek and B. Taccardi (1989). Diagnostic body surface potential map patterns in left ventricular hypertrophy during PQRST. *Am J cardiol* 63(9): 610-7.

Kornreich, F., T. J. Montague, P. Smets, P. M. Rautaharju and M. Kavadias (1989). Multigroup diagnostic classification using body surface potential maps. *Computers in Cardiology*, Jerusalem, Israel.

Leijdekkers, P., V. Gay and E. Barin (2009). Trial results of a novel cardiac rhythm management system using smart phones and wireless ECG sensors. *7th International Conference on smart homes and health telematics*, Tours, France.

Lekkala, J., T. Salpavaara, J. Verho and J. Riistama (2010). Simple inductively coupled resonance sensor for ECG and heart rate monitoring. *Procedia Engineering* 5: 1438-41.

Levy, D., R. J. Garrison, D. D. Savage, W. B. Kannel and W. P. Castelli (1990). Prognostic implications of echocardiographically determined left ventricular mass in the Framingham Heart Study. *N Engl J Med* 322: 1561-6.

London, M., M. Hollenberg, M. Wong, L. Levenson, J. Tubau and W. Browner (1988). Intraoperative myocardial ischemia: localization by continuous 12-lead electrocardiography. *Anesthesiology* 69: 232-41.

MacFarlane, P. W. and T. D. W. Lawrie, Eds. (1989). Comprehensive electrocardiology: Theory and practise in health and disease. Aylesbury, Bucks, England, Pergamon Press.

Malan, D., T. Fulford-Jones, M. Welsh and S. Moulton (2004). CodeBlue: An ad hoc sensor network infrastructure for emergency medical care. *Mobisys, Workshop on Applications of Mobile Embedded Systems (WAMES)*, Boston, MA.

Malmivuo, J. and R. Plonsey (1995). Bioelectromagnetism. Principles and applications of bioelectric and biomagnetic fields. New York, Oxford University Press.

Malmqvist, K., T. Kahan, S. Erikkson, I. Björkander, C. Held, L. Forslund, N. Rehnqvist and P. Hjemdahl (2000). Evalution of various electrocardiographic criteria for left ventricular hypertrophy in patients with stable angina pectoris: influence of using modified limb electrodes. *Clin Physiol* 21(2): 196-207.

Marculescu, P. K. D. and R. Marculescu (2002). Challenges and opportunities in electronic textiles modeling and optimization. *39th ACM/IEEE Design Automation Conference*, New Orleans, LA, USA.

Martin, J. E. T., M. Jones and R. Shenoy (2003). Towards a design framework for wearable electronic textiles. *7th IEEE International Symposium on Wearable Computers (ISWC'03)*, White Plains, New York, USA.

Mason, R. and I. Likar (1966). A new system of multiple-lead exercise electrocardiography. *Am Heart J* 71: 196-205.

Mason, R. E., I. Likar, R. O. Biern and R. S. Ross (1967). Multiple lead exercise electrocardiography: experience in 107 normal subjects and 67 patients with angina pectoris, and comparison with coronary cinearteriography in 84 patients. *Circulation* 36: 517-25.

Mathew, J., P. Sleight, E. Lonn, D. Johnstone, J. Pogue, Q. Yi, J. Bosch, B. Sussex, J. Probstfield and S. Yusuf (2001). Reduction of Cardiovascular Risk by Regression of Electrocardiographic Markers of Left Ventricular Hypertrophy by the Angiotensin-Converting Enzyme Inhibitor Ramipril. *Circulation* 104(14): 1615-21.

McFee, R. and F. D. Johnston (1953). Electrocardiographic leads I. Introduction. *Circulation* 8(10): 554-68.

McFee, R. and F. D. Johnston (1954)[a]. Electrocardiographic leads II. Analysis. *Circulation* 9(2): 255-66.

McFee, R. and F. D. Johnston (1954)[b]. Electrocardiographic leads III. Synthesis. *Circulation* 9(6): 868-80.

Medtronic, Reveal. Retrieved 12.06.2012, from http://www.medtronic.com/for-healthcare-professionals/products-therapies/cardiac-rhythm/cardiac-monitors-insert/reveal-dx-and-reveal-xt-insertable-cardiac-monitors-icms/index.htm.

Michaelides, A. P., Z. D. Psomadaki, P. E. Dilaveris, D. J. Richter, G. K. Andrikopoulos, K. D. Aggeli, C. I. Stefanadis and P. K. Toutouzas (1999). Improved detection of coronary artery disease by exercise electrocardiography with the use of right precordial leads. *N Engl J Med* 340: 340-5.

Miller, T., K. Desser and M. Lawson (1987). How many electrocardiographic leads are required for exercise treadmill tests? *J Electrocardiol* 20: 131-7.

MobiHealth. Retrieved 06.06.2012, from http://www.mobihealth.org/.

Mohammed, O. A. and F. G. Üler (1993). Detailed 2-D and 3-D Finite Element Modeling of the Human Body for the Evaluation of Defibrillation Fields. *IEEE Trans Magn* 29(2): 1403-6.

Munshi, M. C., X. Xiaoyuan, Z. Xiaodan, E. Soetiono, T. Chang Sheng and L. Yong (2008). Wireless ECG plaster for body sensor network. *5th International Summer School and Symposium on Medical Devices and Biosensors. ISSS-MDBS 2008*, Hong Kong, China.

Nadeau, R., P. Savard, R. Guljarani, R. Cardinal, F. Molin and P. Page (1995). Clinical applications of BSM. *J Electrocardiol* 28(4): 334-5.

NASA, Lifeguard system. Retrieved 06.06.2012, from http://www.nasa.gov/centers/ames/research/technology-onepagers/life-guard.html.

Nieminen, T., R. Lehtinen, J. Viik, T. Lehtimaki, K. Niemela, K. Nikus, M. Niemi, J. Kallio, T. Koobi, V. Turjanmaa and M. Kahonen (2006). The Finnish Cardiovascular Study (FINCAVAS): characterising patients with high risk of cardiovascular morbidity and mortality. *BMC Cardiovascular Disorders* 6(1): 9.

National Library of Medicine, Visible Human Project. Retrieved 17 March, 2006, from http://www.nlm.nih.gov/research/visible/visible_human.html.

Nordic Semiconductor. Retrieved 06.06.2012, from http://www.nordicsemi.com/.

Norman, J., James E. and D. Levy (1995). Improved electrocardiographic detection of echocardiographic left ventricular hypertrophy: results of a correlated data base approach. *J Am Coll Cardiol* 26(4): 1022-9.

Novosense AB. Retrieved 06.06.2012, from http://www.novosense.se/technology.htm.

Nöjd, N., M. Puurtinen, P. Niemenlehto, A. Vehkaoja, J. Verho, T. Vanhala, J. Hyttinen, M. Juhola, J. Lekkala and V. Surakka (2005). Wireless wearable EMG and EOG measurement system for psychophysiological applications. *IFMBE Proceedings of the 13th Nordic Baltic Conference on Biomedical Engineering and Medical Physics*, Umeå, Sweden.

Oikarinen, L., M. Karvonen, M. Viitasalo, P. Takala, M. Kaartinen, J. Rossinen, I. Tierala, H. Hänninen, T. Katila, M. S. Nieminen and L. Toivonen (2004). Electrocadiographic assessment of left ventricular hypertrophy with time-voltage QRS and QRST-wave areas. *J Hum Hypertens* 18(33-40).

Okin, P. M., R. B. Devereux, S. Jern, S. E. Kjeldsen, S. Julius, M. S. Nieminen, S. Snapinn, K. E. Harris, P. Aurup, J. M. Edelman and B. Dahlof (2003). Regression of Electrocardiographic Left Ventricular Hypertrophy by Losartan Versus

Atenolol: The Losartan Intervention For Endpoint Reduction in Hypertension (LIFE) Study. *Circulation* 108(6): 684-90.

Okin, P. M., M. J. Roman, R. B. Devereux and P. Kligfield (1995). Electrocardiographic identification of increased left ventricular mass by simple voltage-duration products. *J Am Coll Cardiol* 25(2): 417-23.

Okin, P. M., M. J. Roman, R. B. Devereux and P. Kligfield (1996). Time-Voltage Area of the QRS for the Identification of Left Ventricular Hypertrophy. *Hypertension* 27(2): 251-8.

Omron Healthcare Europe B.V. Retrieved 06.06.2012, from http://www.omron-healthcare.com/en/product/electro_cardiograph/HCG-801-E.html#.

Panescu, D., J. G. Webster, W. J. Tompkins and R. A. Stratbucker (1995). Optimization of cardiac defibrillation by three-dimensional finite element modeling of the human thorax. *IEEE Trans Biomed Eng* 42(2): 185-92.

Polar Electro. Retrieved 06.06.2012, from http://www.polar.fi/en.

Puurtinen, H.-G., J. Hyttinen, P. Kauppinen, J. Nousiainen and J. Malmivuo (1999). Including anatomical changes due to cardiac function into a model of a human thorax as volume conductor. *Nordic-Baltic Conference on Biomedical Engineering*, Tallinn, Estonia.

Puurtinen, H.-G., J. Hyttinen, P. Kauppinen, N. Takano, P. Laarne and J. Malmivuo (2001). Application of lead field theory and computerized thorax modeling for the ECG inverse problem. *Proceedings of the 23rd Annual International Conference of the IEEE Engineering in Medicine and Biology Society, EMBS 2001*, Istanbul, Turkey.

Puurtinen, M., A. Cömert, N. Nöjd, A. Vehkaoja, J. Lekkala and J. Hyttinen (2005)[a]. Wireless wearable bioelectric measurement systems for applications of physiological monitoring and computer interaction. *International Scientific Conference of Intelligent Ambience and Well-Being*, Tampere, Finland.

Puurtinen, M., J. Hyttinen and J. Malmivuo (2005)[b]. Effect of interelectrode distance on measuring sensitivity for facial EMG. *13th Nordic Baltic Conference on Biomedical Engineering and Medical Physics*, Umeå, Sweden.

Puurtinen, M., S. Komulainen, P. Kauppinen, J. Malmivuo and J. Hyttinen (2006). Measurement of noise and impedance of dry and wet textile electrodes, and textile electrodes with hydrogel. *28th Annual International Conference of the IEEE Engineering in Medicine and Biology Society*, New York, USA.

Rautaharju, P. M., T. A. Manolio, D. Siscovick, S. H. Zhou, J. M. Gardin, R. Kronmal, C. D. Furberg, N. O. Borhani and A. Newman (1996). Utility of New

Electrocardiographic Models for Left Ventricular Mass in Older Adults. *Hypertension* 28(1): 8-15.

Riistama, J., J. Väisänen, S. Heinisuo, H. Harjunpää, S. Arra, K. Kokko, M. Mäntylä, J. Kaihilahti, P. Heino, M. Kellomäki, O. Vainio, J. Vanhala, J. Lekkala and J. Hyttinen (2007). Wireless and inductively powered implant for measuring electrocardiogram. *Med Biol Eng Comput* 45(12): 1163-74.

Romhilt, D. W. and E. Estes (1968). A point score system for the ECG diagnosis of left ventricular hypertrophy. *Am Heart J* 75: 751-8.

Russell, J. K. and S. Gehman (2007). Early experience with a novel ambulatory monitor. *J Electrocardiol* 40(6 Suppl): S160-4.

Sarkar, S., D. Ritscher and R. Mehra (2008). A detector for a chronic implantable atrial tachyarrhytmia monitor. *IEEE Trans Biomed Eng* 55(3): 1219-24.

Schillaci, G., P. Verdecchia, C. Borgioni, A. Ciucci, M. Guerreri, I. Zampi, M. Battistelli, C. Bartoccini and C. Porcellati (1994). Improved electrocardiographic diagnosis of left ventricular hypertrophy. *Am J Cardiol* 74(4): 714-9.

Schillaci, G., P. Verdecchia, C. Porcellati, O. Cuccurullo, C. Cosco and F. Perticone (2000). Continuous relation between left ventricular mass and cardiovascular risk in essential hypertension. *Hypertension* 35: 580-6.

Sensatex. Retrieved 06.06.2012, from www.sensatex.com.

Simoons, M. L. (1989). Exercise electrocardiography and exercise testing. Oxford, Pergamon Press.

Texas Instruments, SimpliciTi. Retrieved 06.06.2012, from http://www.ti.com/simpliciti.

SMART: Scalable Medical Alert and Response Technology. Retrieved 06.06.2012, from http://smart.csail.mit.edu/.

Sokolow, M. and T. P. Lyon (1949). The ventricular complex in left ventricular hypertrophy as obtained by unipolar precordial and limb leads. *Am Heart J* 37(2): 161-86.

Song, Z., J. Jenkins, M. Burke and R. Arzbaecher (2004). The feasibility of ST-segment monitoring with a subcutaneous device. *J Electrocardiol* 37 Suppl: 174-9.

Spitzer, V. M., M. J. Ackerman, A. L. Scherzinger and D. G. Whitlock (1996). The visible human male: a technical report. *J Am Med Inform Assoc* 3(2): 118-30.

Spitzer, V. M. and D. G. Whitlock (1997). Atlas of the Visible Human Male. Reverse engineering of the human body, Jones & Bartlett press.

Statistics Finland. Retrieved 06.06.2012, from http://www.stat.fi/til/ksyyt/2009/ksyyt_2009_2010-12-17_tie_001_en.html.

Stern, S. (2002). State of the art in stress testing and ischaemia monitoring. *Card Electrophysiol Rev* 6: 204-8.

St Jude Medical, Confirm. Retrieved 13.06.2012, from http://www.sjmprofessional.com/Products/US/Implantable-Cardiac-Diagnostics/SJM-Confirm-Implantable-Cardiac-Monitor.aspx.

Suunto. Retrieved 06.06.2012, from http://www.suunto.fi/.

Takano, N. (2002). Reduction of ECG Leads and Equivalent Sources Using Orthogonalization and Clustering Techniques, Tampere University of Technology. Doctoral Dissertation.

Tomašić, I., R. Trobec and V. Avbelj (2010). Multivariate linear regression based synthesis of 12-lead ECG from three bipolar leads. *Third International Conference on Health Informatics, HEALTHINF 2010*, Valencia, Španjolska.

Trobec, R., M. Depolli and V. Avbelj (2010). Wireless network of bipolar body electrodes. *Seventh International Conference on Wireless On-demand Network Systems and Services (WONS).* Kranjska Gora, Slovenia.

Trobec, R. and I. Tomas (2011). Synthesis of the 12-lead electrocardiogram from differential leads. *IEEE Trans Inf Tech Biomed* 15(4): 615-21.

Tucker, S., E. Kemp, W. Holland and J. Horgan (1976). Multiple lead ECG submaximal treadmill exercise test in angiographically documented coronary artery disease. *Angiology* 27: 149-56.

Ueno, A., Y. Akabane, T. Kato, H. Hoshino, S. Kataoka and Y. Ishyiama (2007). Capacitive sensing of electrocardiogram potential through cloth from the dorsal surface of the body in a supine position: a preliminary study. *IEEE Trans Biomed Eng* 54(4): 759-66.

Ueshima, K., N. kobayashi, J. Kamata, M. Saitoh, T. Yamazaki, I. Chiba and K. Hiramori (2004). Do the right precordial leads during exercise testing contribute to detection of coronary artery disease? *Clin Cardiol* 27(2): 101-5.

Uhari, M. and P. Nieminen (2001). Epidemiologia ja biostatistiikka. Helsinki, Duodecim.

Wagner, G. S. and H. J. L. Marriott (2007). Marriott's practical electrocardiography. Philadelphia, Lippincott, Williams and Wilkins.

Walker, S. J. (1985). Epicardial potential distributions calculated from body surface measurements using multiple torso models, University of Tasmania. Doctoral Dissertation.

Walker, S. J. and D. Kilpatrick (1987). Forward and inverse electrocardiographic calculations using resistor network models of the human torso. *Circ Res* 61(4): 504-13.

Vehkaoja, A., J. Verho, A. Cömert, B. Aydogan, M. Perhonen, J. Lekkala and J. Halttunen (2008). System for ECG and heart rate monitoring during group training. *30th Annual International Conference of the IEEE Engineering in Medicine and Biology Society, IEEE EMBS, Personalized Healthcare through Technology*, Vancouver, British Columbia, Canada.

Vehkaoja, A., J. Verho, M. Puurtinen, N. Nöjd, J. Lekkala and J. Hyttinen (2005)[a]. Wireless head cap for EOG and facial EMG measurements. *27th Annual International Conference of the IEEE Engineering in Medicine and Biology Society*, Shanghai, China.

Vehkaoja, A., J. Verho, M. Puurtinen, N. Nöjd, J. Lekkala and J. Hyttinen (2005)[b]. Wireless input device for hands-free computer-human interaction. *International Scientific Conference of Intelligent Ambience and Well-Being*, Tampere, Finland.

Wendel, K. E. (2010). The influence of tissue conductivity and head geometry on EEG measurement sensitivity distributions, Tampere University of Technology. Doctoral dissertation.

WHO (2008). The World Health Report 2008 - primary Health Care (Now More Than Ever). Geneva, World Health Organization.

Wierzbowska, K., M. Kurpesa, J. Peruga, J. Drozdz, M. Krzeminska-Pakula and J. Kasprzak (2002). Role of the right chest lead in improving the accuracy of myocardial ischemia detection. *Przegl Lek* 59(9): 684-6.

Viik, J. (2000). Diagnostic properties of exercise electrocardiographic leads and variables in the detection of coronary artery disease, Tampere University of Technology. Doctoral dissertation.

Viik, J., R. Lehtinen, V. Turjanmaa, K. Niemelä and J. Malmivuo (1997). The effect of lead selection on traditional and heart rate-adjusted ST segment analysis in the detection of coronary artery disease during exercise test. *Am Heart J* 134: 488-94.

Viik, J., R. Lehtinen, V. Turjanmaa, K. Niemelä and J. Malmivuo (1998). Correct utilization of exercise electrocardiographic leads in differentiation of men with coronary artery disease from patients with a low likelihood of coronary artery disease using peak exercise ST-segment depression. *Am J Cardiol* 81: 964-9.

Väisänen, J. (2010). Methods for analysing the sensitivities of bioelectric measurements, Tampere University of Technology. Doctoral Dissertation.

Väisänen, J., J. Hyttinen and J. Malmivuo (2006). Analysing specificity of a bipolar ECG implant to 12 segments of the left ventricle. *Computers in Cardiology*, Valencia, Spain.

Väisänen, J., J. Hyttinen and J. Malmivuo (2006). Finite difference and lead field methods in designing implantable ECG monitor. *Med Biol Eng Comput* 44(10): 857-64.

Väisänen, J., M. Puurtinen, J. Hyttinen and J. Viik (2010). Short distance bipolar electrocardiographic leads in diagnosis of left ventricular hypertrophy. *Computing in Cardiology*, Belfast, Northern Ireland, United Kingdom.

Väisänen, O. (2008). Multichannel EEG methods to improve the spatial resolution of cortical potential distribution and the signal quality of deep brain sources. Tampere, Finland, Tampere University of Technology. Doctoral Dissertation.

Zephyr Technology Corp. Retrieved 06.06.1012, from http://www.zephyr-technology.com/.

ZigBee Alliance. Retrieved 06.06.2012, from http://www.zigbee.org/.

9. ORIGINAL PUBLICATIONS

Tampereen teknillinen yliopisto
PL 527
33101 Tampere

Tampere University of Technology
P.O.B. 527
FI-33101 Tampere, Finland

ISBN 978-952-15-2896-5
ISSN 1459-2045